MODELING MULTIPLE OBJECT SCENARIOS FOR FEATURE RECOGNITION AND CLASSIFICATION USING CELLULAR NEURAL NETWORKS

Tendani Calven Malumedzha

A Dissertation submitted to the Faculty of Engineering and Built Environment, University of the Witwatersrand, in fulfillment of the requirements of the degree of Master of Science in Engineering

Johannesburg 2009

MODELING MULTIPLE OBJECT SCENARIOS FOR FEATURE RECOGNITION AND CLASSIFICATION USING CELLULAR NEURAL NETWORKS

by

ABSTRACT

Cellular neural networks (CNNs) have been adopted in the spatio-temporal processing research field as a paradigm of complexity. This is due to the ease of designs for complex spatio-temporal tasks introduced by these networks. This has led to an increase in the adoption of CNNs for on-chip VLSI implementations. This dissertation proposes the use of a Cellular Neural Network to model, detect and classify objects appearing in multiple object scenes. The algorithm proposed is based on image scene enhancement through anisotropic diffusion; object detection and extraction through binary edge detection and boundary tracing; and object classification through genetically optimised associative networks and texture histograms. The first classification method is based on optimizing the space-invariant feedback template of the zero-input network through genetic operators, while the second method is based on computing diffusion filtered and modified histograms for object classes to generate decision boundaries that can be used to classify the objects. The primary goal is to design analogic algorithms that can be used to perform these tasks. While the use of genetically optimized associative networks for object learning yield an efficiency of over 95%, the use texture histograms has been found very accurate though there is a need to develop a better technique for histogram comparisons. The results found using these analogic algorithms affirm CNNs as well-suited for image processing tasks.

Declaration

I declare that this dissertation was composed by myself, that the work contained herein is my own except where explicitly stated otherwise in the text, and that this work has not been submitted for any other degree or professional qualification except as specified.

.....

Tendani Calven Malumedzha

Acknowledgements

Special thanks to my supervisors Prof. Tshilidzi Marwala and Dr. Vincent Nelwamondo for a great deal of time i spent under their guidance. Their confidence in me was an inspiration. I also thank Dr. Anthony Gidudu for a good introduction to satellite imaging and applications, which gave more purpose and direction to my research.
Thanks to my beloved parents Mr C. Malumedzha and Mrs D. Malumedzha for the undying support, encouragement and patience they have shown me during my research. They have shown me that they believe in what i do. I also thank my Atos Origin SA VAS colleagues for some intellectual and challenging conversations that have always kept me on the edge. I also wish to acknowledge Themba and Tshepo for the support and guidance they have given me since i joined Atos Origin SA.
Lastly, i thank God for giving me the strength to work through even with the challenges that i have been facing during this research.

to my parents, Colbert and Dorcus Malumedzha

Contents

List of Figures

Chapter 1

Introduction

1.1 Artificial Object Modeling and Complexity

The human visual system is equipped with a highly intelligent technique to segment and distinguish between multiple objects appearing in one visual scene. With this technique, the human eye can perform segmentation and extraction, classification, tracking and recognition tasks to a very high degree of accuracy. There are however limitations in this accurate system, which are normally a result of the state of the human brain, which is prone to the disturbances such as emotional reactions, tiredness etc. With these disturbances it becomes a challenge for a human eye to monitor a visual task or process constantly while making correct decisions at all times. For this reason, science and engineering have found it important to model the behaviour and processing techniques employed in the human visual system through Artificial Intelligence (AI) and visual capturing tools implemented into an artificial visual processor.

As industrialization of engineering processes grows, it is accompanied by the growing need to monitor the processes through visual robots capable of detecting errors and defects that can hamper productivity in the process. The visual robots also serve as a quality assurance method as defective materials and/or erroneous behaviour in the process are detected as they happen and corrected before they impact on profits/performance. The use of these online visual tools also provide an added advantage in case the raw material of the process could have been reusable if the process was

stopped just in time the material becomes defective.

The recent growth in urbanization, land cover/use changes, climatic changes and increased security surveillance require highly intelligent and sophisticated tools for analysis and study. For these tasks to be carried out, there is a need to perform object detection, segmentation, extraction or classification. This is achieved through the design of models that accurately represent the object artificially. Object modeling for visual processing in a computer is a complex process that require certain mathematical formulation to describe the dynamics of the object. This dissertation will address the following challenges:

(i) designing a mathematical model that represent the dynamics of the object. The model must capture most of the object's features such as shape, colour and texture. This include the ability to map the object spatial data on a one-to-one bases with the model,

(ii) creating a model sensitive to small changes in the object's features(i.e. high spatial and temporal resolutions in the model),

(iii) creating a model less intensive in mathematical computations (i.e. reducing model complexity and designing a model easy to understand),

(iv) restricting the system to consume a reasonable amount of memory and CPU time, and

(v) creating a model that is adaptive.

1.2 AI Approaches to Object Modeling

Modeling objects for image processing tasks has been part of an ongoing research. Though presently advanced and simplified, image processing has been classified as one of the most complex spatio-temporal processes. Traditionally, the nonlinear spatio-temporal computing was achieved by 32-bit floating point digital calculations on nonlinear Partial Differential Equations (PDEs); this is a complex problem to solve even with digital supercomputers [1]. There are several disadvantages that are inherent in linear PDE methods, these include mathematical intensiveness and the difficulty in

achieving an accurate mapping of the spatial and temporal parameters of the model to those of the problem being modeled [1].

AI approaches have been seen to yield advantages over classical mathematical approaches, with the overall performance of over 90% in visual computing tasks [2]. Among these techniques is the application of Artificial Neural Networks (ANN), Fuzzy logics, Markov Random Fields (MRF) and agent-based models to capture the object features into the model. The inherent problems with the use of these methods are the complexity of the algorithms and the sacrifice in processing speed when Very Large Scale System Integration (VLSI) chips are implemented [3]. An integration of on-chip sensors and array computers to process real time signals originating from space distributed sources (e.g. images and videos) using traditional neural architectures such as the Hopfield Networks and Kohonen's Self-Organized Feature-Mapping (SOFM) algorithms presents implementation difficulties as these architectures are not well suited to nonlinear spatio-temporal computing [3][4].

In view of the above, more focus was directed to the design of analog-based processors with analogic instead of digital computational capabilities. A major breakthrough came in 1988, when Chua and Yang [5] presented their work on a Cellular Neural Networks (CNNs) architecture.

1.3 CNNs as a Platform for Spatio-temporal Processing

Cellular Neural Networks are composed of cells that are coupled together to form a dynamic nonlinear array. Each cell in the array is a dynamical system on its own and exhibits a specific behaviour that is related to the neighbouring cells through rules defined between each cell and its neighbours. In the initial formulation of the model, CNNs are defined as a model of complexity [6]. The formulation was also inspired by the model of universal complexity from the smallest particle of matter, *the cell*, in which it is argued that the complexity of the universe can be made easier through understanding the behaviour of a cell, i.e modeling and computing the dynamics of the cell and using coupling rules between cells to propagate the overall dynamical behavior of the cells forming the universe [7].

Due to its array nature, the CNN model gives a platform of computation for data that is

distributed in both space and time, i.e. *spatio-temporal data*. CNNs are *analogic* arrays, possessing both the fast computing nature of analog circuits and the logic nature that defines the circuit rules in their digital counterparts. Each cell in a CNN array is a processor, this makes CNNs more suited to parallel and synchronous processing and hence the ideal candidates for VLSI implementation. A CNN cell is only coupled with its neighbours, thus suggesting that the processing in the network is local and hence the decreased mathematical computation and model complexity. There is also a one-to-one mapping between a CNN cell and the pixel on the image being modeled [8]. Amongst many other advantages, the behaviour of the CNN can be easily altered by changing the coupling rules modeled as the cloning template of the CNN. Figure 1.1 shows a CNN array with cell interactions [9].

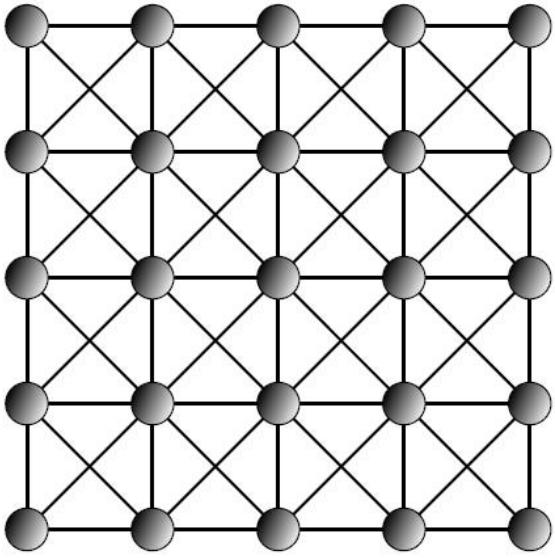

Figure 1.1: A CNN array with 9 neighbouring Cells [9]

1.4 Contribution to Research

The main contribution of this dissertation is on the formulation of an approach to solve the spatio-temporal problem of object modeling for the purpose of detection,

segmentation, extraction and classification in multiple object scenes with emphasis to reduce model complexity, increase computational speed and create an easy-to-implement method of training and classification using CNNs. To achieve this contribution we address the problems stated in section 1.1. The inspiration to undertake this research was derived from an observation that most existing spatio-temporal solutions do not address the problem of complexity of the model. There is also a rising need to implement visual processing tasks on-chip, which in turn demands that the model complexity is reduced in order to work in harmony with the chip resources. The reduction of the model complexity involves choosing a modeling technique that best suits the application, and the best algorithm that increases memory efficiency and computational speed while maintaining high accuracy. For this reason, Cellular Neural Networks (CNN) were chosen as a platform for computing. Through examining the reported work in the field of CNNs, it was noted that there has not been more focus on the methods of handling classification of multiple objects/features appearing on one image scene [63]. The available work only lay foundations as to how isolated objects can be classified, but however does not take into account that learning object features may be more effective if the environment in which the object appears in is taken into account. This document formulates the techniques in the Cellular Neural Network domain that can be used to achieve models of the objects and the application of optimisation techniques to improve the model performance for applications in object detection, extraction and classification based on multiple object scenes.

1.5 Objectives

This document proposes the methods of handling object modeling and computation in multiple object scenarios for the purpose of detection, segmentation, extraction and classification. Within this main objective, there are several sub-objectives that must be fulfilled. The following are the sub-objectives through which the main objective is achieved:

(a) define multiple object classification in terms of modeling and complexity. This gives answers to the possible causes of model complexity and how artificial intelligent techniques can be employed to reduce the complexity.

(b) device techniques through which an efficient object model can be achieved and accounted for. This follows an exploration of possible CNN techniques that can be integrated to yield an algorithm that can solve the problem defined on the point above. This involves evaluation of certain approaches and the adoption of others owing to their suitability and applicability to spatio-temporal modeling.

(c) formulate optimisation techniques that best optimizes the object models achieved by the chosen modeling technique. Selecting the best method for optimization implies the achievement of a global solution that best captures all the object traits. A selection of an inadequate method result in the solution trapped in local maxima.

(d) to create an easy-to-implement algorithm for the training and classification of objects modeled using CNNs. This will serve to indicate the possible advantages of the choice of CNNs as the proper model for the application of object detection, extraction and classification.

(e) design an object-based algorithm that consists of reusable parts for all tasks i.e. segmentation, extraction and classification. This means that a task that is required by both CNN based image processing tasks is implemented in a polymorphic approach.

(f) integrate all the algorithm parts into a single analogic framework that defines how multiple object scenarios are handled using CNNs.

(g) develop a proof-of-concept application that demonstrates the strength of the algorithm proposed in this research work. This objective seeks to demonstrate how the proposed methods can be applied to solve practical problems.

(h) develop an analysis procedure that is to be used to determine the performance of the model. Here the accuracy, efficiency and resource intensiveness of the proposed methods are determined in order to numerically scale their performance.

1.6 Chapters and their Respective Contribution

This dissertation is organized into chapters each serving one or more objectives detailed above. While Chapter 2 builds up a background required to understand the main direction of this research, the rest of the chapters build up the solution to the problem of multiple object scenario handling, with each chapter focusing on a specific building block of the entire solution proposed. The following is a brief discussion on the content and objectives of each chapter:

1. **Chapter 2** gives a thorough background to CNNs. In this chapter the CNN architecture and its dynamics are presented. The suitability of the architecture to the spatio-temporal applications is explored and its limitations in general. This will involve a look at some practical images and their corresponding CNN models.

2. **Chapter 3** The objective of this chapter is to formulate and present a series of CNN based image processing tasks that allow the object to be separated from the background and other objects in the image without altering its features. In order to achieve this we employ image processing methods such as nonlinear diffusion, CNN based thresholding and edge detection. A successful extraction technique leads to the image model that can be used during learning and classification.

3. **Chapter 4** presents various strategies that can be used to select the features that best represent the object being studied. This chapter deals mainly with how the object features are represented as sets of stable memories and stored in the CNN templates. This chapter also presents the types of CNN networks that can be used for learning object features. Several features that are regarded as more distinctive to objects will also be examined. Of this we study texture through texture histograms and apply heuristics to design bounds for texture classes.

4. **Chapter 5** is an integration of all the chapters above into analogic algorithms that can be used to train the CNN to classify objects. The algorithm proposed here is general and can be adopted to different application scenarios. Two algorithms are proposed, namely (1) genetically optimized CNNs for feature learning and texture histograms for boundary conditions design for class objects.

5. **Chapter 6** gives an introduction to some practical examples where the proposed algorithms are applicable. Example 1 is a practical application of the algorithm designed during this research and submitted to the International Association of Science and Technology for Development(IASTED). This example is in the classification of satellite sensed data using genetically optimized CNNs. Another example presented is on the use of diffusion filtered and modified histograms to perform texture based classification of objects based on multiple texture object scenes. This chapter further details the analysis procedure to be used to evaluate the performance of the algorithms proposed in this document. The procedure involves setting up certain standards of acceptability for any algorithm in this case by looking at measures of efficiency such as memory utilisation, processing time, percentage accuracy and applicability in real world problems.

6. **Chapter 7** summarizes all the chapters by looking back at the goals set in section 1.5. It further details the impact of this research to the modern world and paves way to challenges in this research that require further investigation. The chapter also gives the weight of the material covered in this research in terms of originality and referencing.

Chapter 2

CNNs in Image Processing

2.1 Local Processing, Coupling and Nonlinear Dynamics

In the introduction of the CNNs a paradigm of complexity, a CNN is defined as a regular array of MXN dimensions composed of nonlinear units with only local interaction within a neighbourhood radius [5,6]. The most distinctive features of this model are [8]:

1. **local processing**, which ensures that all cell interactions are local (i.e. within each cell and its neighbours). This decreases the complexity of the model.

2. **coupling**, defines the rules of cell interactions within the neighbouring cells. The behavior of the network is altered by changing these rules. The complexity of the model increases if there is no coupling in the network. Uncoupled cells in an array can present chaos and instability. The relational rules for mapping input and output becomes difficult to model and define when there is no inter-relationships between local cells [9].

3. **nonlinear dynamics**, define the nature of the processing elements, the cells. "dynamic" implies the dependency of the cells on the state of the neighbouring cells, while "nonlinear" defines the nature of the output activation caused by the Chua-Yang's choice of the piecewise-linear function.

In analogy to the universe, *local processing* describes the dynamics and functioning of the smallest building blocks of matter, the cells, while *coupling* defines the the influence

that neighbouring cells have on the state of the cell and propagation of the cell behaviour throughout the entire universe to give it an overall dynamic behavior. Through coupling and local interaction, the dynamics of very complex nonlinear systems can be modeled and analysed. Section 2.2 introduces one of such models for complexity introduced by Chua and Yang in [5].

2.2 The Chua-Yang CNN Model

The idea proposed by Chua and Yang to address the problem of complexity was to use an array of dynamical cells to process a large amount of data in real time [1]. Processing data in real time require analog processors, while processing large amounts of data may require parallel synchronous processors. This supports their choice of a cellular array wherein each cell is an analog processor that serves as an input-output stage of the network. In order to control the behaviour of the model with respect to the dynamic range and stability, Chua and Yang apply logic theory that is widely used in digital circuits. This result into a computer that possesses both the speed and computational power of analogue and digital circuits, which is presently known as the *Analogic Computer*[10].

In the original Chua-Yang model, the neighbourhood, r, of a dynamical cell in the i-th row and the j-th column, termed C_{ij}, on an $M\ X\ N$ CNN array is defined by:

$$N_{ij}^{r} = \{\ C_{kl} | max\{|k-i|, |l-j|\} \geq r;\quad 1 \leq k \leq N_1, 1 \leq l \leq N_2\} \tag{2.1}$$

where r is a positive integer, and i and j are row and column indexes respectively [5,6,7,10].

Each cell of the CNN has a continuous valued state variable x, an input variable u, and the output y. The nonlinear dynamics of the CNN is defined by the following set of equations:

$$C\frac{dx_{ij}(t)}{dt} = -\frac{1}{R}x_{ij}(t) + \sum_{C_{kl}\epsilon N_{ij}^{r}} A(i,j;k,l)y_{kl}(t) + \sum_{C_{kl}\epsilon N_{ij}^{r}} B(i,j;k,l)u_{kl} + I_{ij}$$

and

$$y_{ij}(t) = \frac{1}{2}(|x_{ij}(t)+1| - |x_{ij}(t)-1|) \tag{2.2}$$

where C and R are integral constants of the system, x_{ij} is the state of a cell, I is an independent bias constant, and y_{ij} is the activation function [5,7].

The matrices A and B that operate on the input and the output respectively are called the Cloning Templates or the CNN Kernel. The former acts as feedback template and the latter as an input control template [5,8,10]. The cloning template represented by A and B may be linear or nonlinear, space variable or invariable depending on the application. The output function of the CNN is chosen based on the desired application of the CNN. [5] and [10] lists the following output activation functions and their areas of application:

1. piecewise-linear model - shown in equation 2.2.
2. nonlinearity model - most applicable to on-chip VLSI
3. hyperbolic function - used for training applications where the learning follows the gradient descent rule.

The activation functions described above are as shown in Figure 2.1.

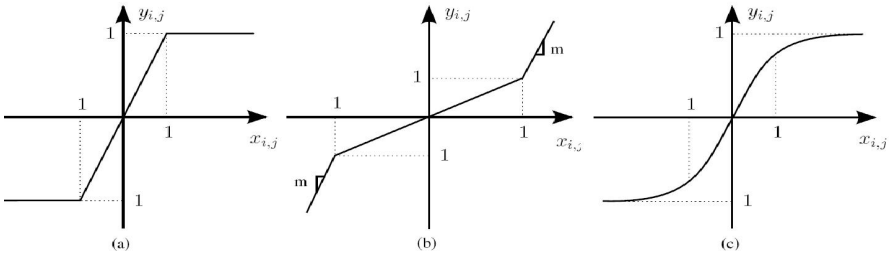

Figure 2.1: The learning functions used in the CNN output activation:(a) the piecewise-linear model, (b) the nonlinearity model and (c) the tangential hyperbolic function [9]

The neural feedback capability of the CNN as controlled by the cloning templates is as shown in Figure 2.2 which shows a block diagram model of a cell, also known as a neuron. The neuron model as seen in the figure has dynamics that are dependent on

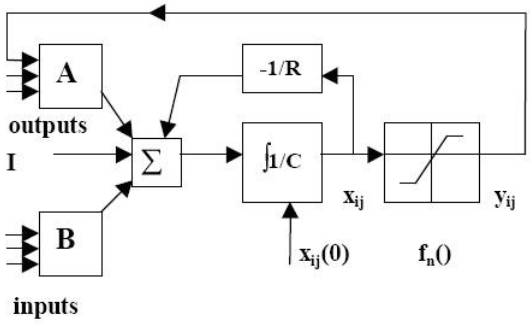

Figure 2.2: The block diagram depicting the signal flow on a CNN Cell [11]

coupling rules set on the templates A and B.

The number of parameters used to set these rules is determined by the r-neighbourhood chosen for the design. For example, a CNN with neighbourhood $r = 1$ require 9 parameters for both matrices A and B, while the neighbourhood of $r = 2$ require 25 coupling parameters per template operator. Generally the number of parameters in the template can be derived from $(2r+1) \times (2r+1)$, where r is the neighbourhood chosen for the network [5,8,10]. The network complexity increases with the increase in r. Some examples of r-neighbourhood architectures are shown in Figure 2.3.

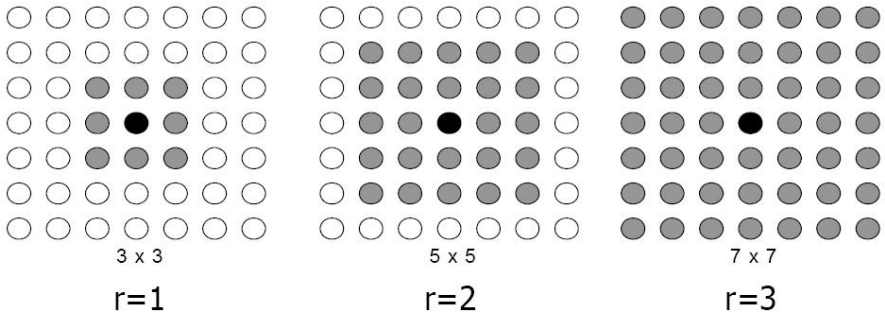

Figure 2.3: The r-neighbourhood representation in the CNN architecture. The dark cells represent the relationship that is considered in achieving a CNN model [10].

2.2.1 CNN Classes

The most categorizing parameter of a CNN is the cloning template . With alteration of the cloning template, a wide range of CNNs with unique behaviours are defined. However, Chua and Roska define three classes from which all the subclasses inherit their behaviour [10].

(a). Zero-Feedback or Feedforward CNNs

A CNN that belongs to this class is defined by the following equation:

$$C\frac{dx_{ij}(t)}{dt} = -\frac{1}{R}x_{ij}(t) + \sum_{C_{kl}\epsilon N_{ij}^{r}} B(i,j;k,l)u_{kl} + I_{ij} \tag{2.3}$$

This class is characterized by an uncoupled behaviour between the input of the network and the corresponding output. The signal flow system structure associated with the cell forming this type of network is shown in Figure 2.4.

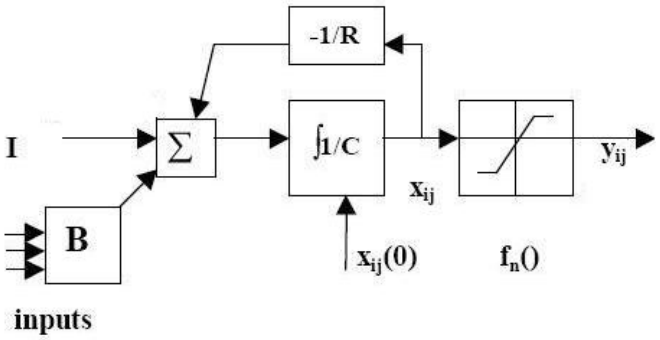

Figure 2.4: The system structure depicting the signal flow of the zero-feedback CNN cell [10]

(b). Zero-Input CNNs

A CNN belonging to this class is defined by equation 2.4. This network does not take any input as there is no input control template (i.e the B template is zero). The input

is supplied to the network as a state signal.

$$C\frac{dx_{ij}(t)}{dt} = -\frac{1}{R}x_{ij}(t) + \sum_{C_{kl}\epsilon N_{ij}^{r}} A(i,j;k,l)y_{kl}(t) + I_{ij} \tag{2.4}$$

The signal flow model followed by a cell belonging to this class is as shown in Figure 2.5.

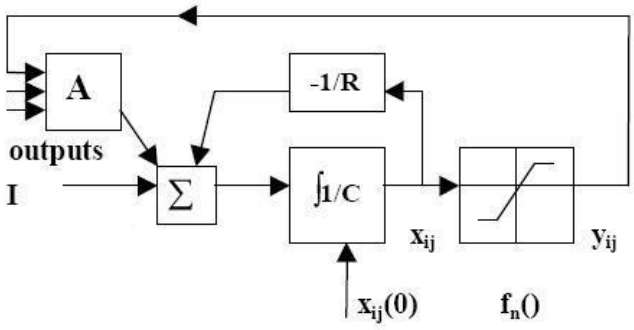

Figure 2.5: The system structure depicting the signal flow of the zero-input CNN cell [10]

(c). Uncoupled CNNs

These networks are defined by equation 2.5. Only the contribution made by that particular cell is fed back to the input. This networks are uncoupled as the effects of the neighbouring cells are ignored when computing the cell dynamics.

$$\frac{dx_{ij}(t)}{dt} = -x_{ij}(t) + a_{00}y_{kl}(t) + \sum_{C_{kl}\epsilon N_{ij}^{r}} B(i,j;k,l)u_{kl} + I_{ij} \tag{2.5}$$

where a_{00} is the template parameter that represents the contribution of that individual cell to the overall output of the CNN.
The signal flow associated with cells of this class is shown in figure 2.6.

2.2.2 Space Invariant CNNs

Generally, both coupled and uncoupled CNNs can have both time and space variable templates. This means that the nature of coupling between a cell and its neighbour is

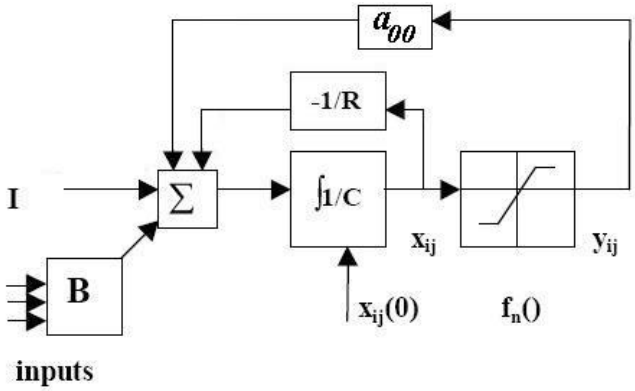

Figure 2.6: The system structure depicting the signal flow of the uncoupled CNN cell [10]

spatially distributed following certain mathematical constraints. The majority of real life applications require that the coupling distribution between the cells in the entire network is invariant, thus demanding that the network template parameters are space invariant [10]. Space invariant networks represent a set networks with cloning template parameters that do not change throughout the propagation of cellular dynamics in the entire array. The matrices in equation 2.6 represent the type of template associated with these networks [12].

$$A = \begin{pmatrix} a_1 & a_2 & a_3 \\ a_4 & a_5 & a_6 \\ a_7 & a_8 & a_9 \end{pmatrix}, \quad B = \begin{pmatrix} b_1 & b_2 & b_3 \\ b_4 & b_5 & b_6 \\ b_7 & b_8 & b_9 \end{pmatrix} \tag{2.6}$$

where a and b are constant values.

2.2.3 Associative Memories in CNN

The goal of associative memories is to store features or attributes of the input for later recollection. A network that has the potential to store attributes of the input is vital in applications such as recognition and classification. For example, in image processing the raw image data is expressed as a set of pixel values that map onto some domain

that may represent an edge or some other features that distinctively characterize the object or one of its class. The goal of an associative processor in this case is to associate any other input that it has never learned with the one of its kind that has been learned. Generation of associative memories in the CNN architecture means the design of coupling rules between each cell and its neighbours that can be stored as kernel maps (template) for the recollection of a particular input pattern [13].

There are several methods of implementing associative memories in CNNs. Szolgay *et al* [14] propose a fixed point learning method for associative memory design with space varying templates. The design is based on the autonomous (Zero-input) CNN model defined in section 2.2.1. The method is based on computing the cost function that provides the best convergence speed. During learning the equilibrium state of a cell should be located outside the region of saturation. For this condition to be sufficient, the magnitude of the equilibrium point is evaluated by equation 2.7.

$$E_{ij}^n = A_{ij}^T.p_{ij}^n + I_{ij}.y_{ij}^n \quad : \quad E_{ij}^n \leq E \leq 1 \tag{2.7}$$

where $n = 1,,,,p;i = 1,,,M;j = 1,,,N$ and E is the constant around which magnitude of an equilibrium point of a cell is set.
With the satisfaction of the condition in equation 2.7, Szolgay *et al* uses the Herbial Lerning Rule to compute the matrix A_{ij} using a weighting factor W_{ij}^n of the nth pattern as shown in equation 2.8.

$$A_{ij} = \sum_{n=1}^{p} W_{ij}^n.p_{ij}^n \tag{2.8}$$

Using the Zero-input network, Liu and Lu [15] propose a procedure for the synthesis of space invariant CNN templates. The design algorithm is based on the eigenstructure method where a set matrices representing cloning template parameters of the Network are derived through singular value decomposition. The method is implemented with a view of the perceptron learning algorithm to ensure convergence at an optimal solution (i.e. termination of algorithm with stable memories)

The synthesis procedure for this approach is based on the discrete time CNN model with the following set equations:

$$\dot{x} = -x_{ij} + T_{ij,kl} sat(x) + I_{ij} \quad where \quad y_{ij} = sat(x) \tag{2.9}$$

where A is chosen to be an identity matrix, $T_{ij,kl}$ is the feedback cloning template and I_{ij} is the threshold or bias current.

There are several comparisons that can be drawn between the CNN associative model and its Hopfield counterpart. While the weights of the hopfield network are computed through a herbian rule, the CNN learning is not limited to any specific rule. The Hopfield model operates asynchronously, whereas the CNN model can operate in a synchronous mode. Due to local connectivity, the interconnection matrix that is required to store the stable memories in the CNN is very small. A fully connected hopfield network require more space to store all interconnection weights between the inputs, hidden layers and the output(s). This comparison is illustrated further in figure 2.7 where the two networks are compared.

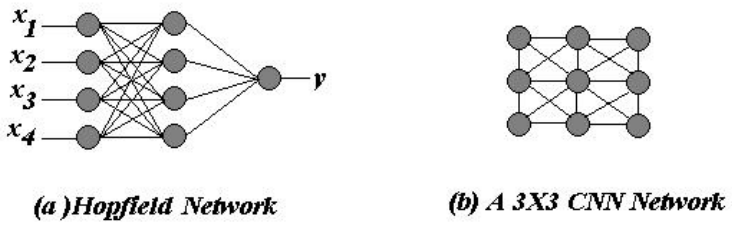

Figure 2.7: (a) A fully Hopfield Network and (b) a 3 X 3 CNN network. A Hopfield of $n = 9$ has a total of 729 interconnections, while a CNN of $n = NXM = 9 \; for \; M = N = 3, \; r = 3$ has a total of 289 interconnections

2.3 The CNN Analogic Algorithm

Analogic algorithms define the processing methods based on analog and logic computing. An analogic algorithm entails a combination or sequence of CNN operators required to

solve a complex problem in real time. For example, the necessary steps required to perform CNN-based image morphology are implemented as a series of CNN operators. Analogic algorithm implies the application of one or more CNN space and/or time variant/invariant template(s) to an input in a predefined sequence and time to generate a spatio-temporal solution. These algorithms are key to the formulation of a CNN based solution to spatio-temporal problems. By altering the cloning templates of a network at specific times and order, the input parameters are processed into some output that is required for the application on the next processing stage. In [10], an example of an analogic algorithm that implements non-separable XOR boolean function is designed as shown in Figure 2.8. In this they show that the XOR can be implemented as a set of sequential analogic expressions each applying a specific template. The primary building blocks of the analogic algorithm herein explored are the logic NOT, logic AND and logic OR which are given by the templates in equations 2.10, 2.11 and 2.12.

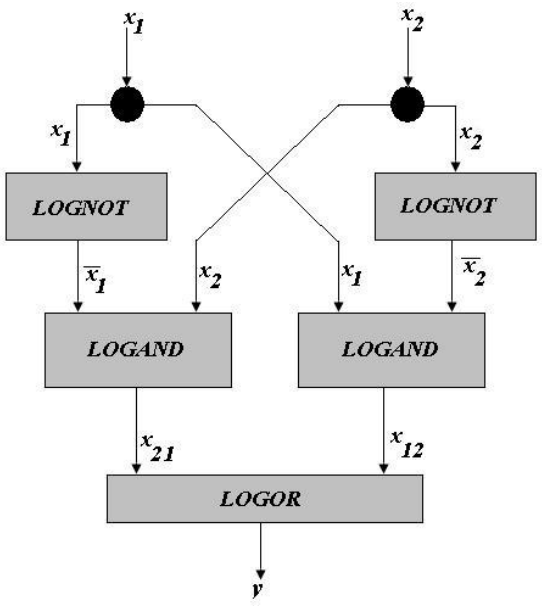

Figure 2.8: The analogic algorithm showing how a non-separable Boolean function XOR is implemented [10]

(i). The logic NOT

$$A = \begin{pmatrix} 0 & 0 & 0 \\ 0 & 1 & 0 \\ 0 & 0 & 0 \end{pmatrix}, \quad B = \begin{pmatrix} 0 & 0 & 0 \\ 0 & -2 & 0 \\ 0 & 0 & 0 \end{pmatrix}, \quad I = 0 \tag{2.10}$$

(ii). The logic AND

$$A = \begin{pmatrix} 0 & 0 & 0 \\ 0 & 2 & 0 \\ 0 & 0 & 0 \end{pmatrix}, \quad B = \begin{pmatrix} 0 & 0 & 0 \\ 0 & 2 & 0 \\ 0 & 0 & 0 \end{pmatrix}, \quad I = -2 \tag{2.11}$$

(iii). The logic OR

$$A = \begin{pmatrix} 0 & 0 & 0 \\ 0 & 2 & 0 \\ 0 & 0 & 0 \end{pmatrix}, \quad B = \begin{pmatrix} 0 & 0 & 0 \\ 0 & 2 & 0 \\ 0 & 0 & 0 \end{pmatrix}, \quad I = 2 \tag{2.12}$$

2.4 The Adoption of the CNN Architectures for Image Processing

Image processing involves the manipulation of the visual and non-visual aspects of an image with a goal of extracting and studying the information contained in it. Image processing is a well developed field and has found application in areas such as visual quality inspection, tracking, pattern recognition and visual classification. Though artificial intelligent models have been found to be more accurate, most of them do not address the problem of complexity, memory and computational speed. The emergence of CNNs have introduced a paradigm of solving complex image processing problems with increased computational speed and reduction of memory utilisation [1].

Since inception, the CNN architecture has been actively researched for application to spatio-temporal processing and industries have witnessed the realisation of VLSI-based visual processors. The simplicity of the CNN architecture has attracted more research for applicability in visual computing. Highly complex image models have been designed using CNNs, for example the CNN retina model [16][17], the DNA microprocessor arrays

[1] and Cellular Wave Computers for Brain-like Spatial-temporal Sensory Computing [18]. Wang *et al* [19] investigated the use of CNNs to perform object segmentation in image sequence, taking advantage of the image statistical data. That is, by mapping the image spatial domain to its statistical domain, a robust image segmentation method can be achieved even in cases of changing background. Szabo and Szolgay [20] have described an analogic-based (CNN) diffusion algorithm for segmentation of image by performing CNN-based binary mathematical morphology. The use of bayesian techniques combined with CNNs has also been proposed by many researchers. Milanova, Elmaghraby and Rubin [11] have discussed the MRF-based method which takes advantage of the Maximum of a posteriori (MAP) and the CNN energy function. This method also tries to map the CNN model of an image onto its statistical representation. There are many CNN templates that exist to handle the image segmentation in different imaging environments.

Various methods of using CNNs in feature extraction and classification have also been reported in many publications. Rekeczky *et al* [21] have developed a framework for a cellular (visual) sensor computer which performs feature detection based on terrain classification; and motion analysis based on navigation parameter estimation. In [22] and [23], Rekeczky *et al* also detail a method of feature extraction by computing topographic feature maps from video terrain flows, feature selection by Principal Component Analysis (PCA) and Decision Trees; and feature classification using Nearest Neighbor Family (NNF) methods.

Optimization techniques have also been deployed to enhance techniques of feature detection in CNN architectures. Vandewalle and Dellaert [24] outline a method for automatic design of CNNs using Genetic Algorithms (GAs) to perform image feature detection. In order to perform classification using CNN templates, a synthesis of autoassociative memory (as in the case of Hopfield Networks) is essential. CNN associative memory for feature recall and classification purposes is achieved through design procedures that try to mimic the nature of associative recall in Hopfield Networks. [14,15,24] and [25] propose a variety of methods such as GAs, fixed-point learning and eigenstructure methods which can be used in template design for associative memories.

These applications unleash CNNs as networks highly suited for complex systems modeling and analysis. In Chapter 3, the use of these networks to derive models for objects

embedded in multiple object scenarios is explored. The accurate models in these case are achieved through accurate detection, segmentation and extraction of the object from the scene in order to study the object in isolation.

Chapter 3

Multiple Object Scenario Modeling using CNNs

This chapter forms the base of the proposed algorithms for dealing with object modeling in multiple object scenes. For the purpose of this chapter, a definition of a "multiple object" scene is outlined first, with emphasis to the inherent complexities in modeling objects in multiple object views. This chapter extends the available methods for the designing analogic algorithms that are suitable for this task. The first step required for a successful model is the filtering stage that normalizes the image and enhance the pixel intensities to ensure consistency. Various techniques of image filtering are introduced. The importance of computing statistical tools such as mean, variance, diffusion and threshold images is also evaluated. The object model is considered accurate if it successfully leads to an accurate extraction of that object from the scene. In this chapter, the focus is mainly on the development of analogic algorithms that output the extracted object. These algorithms are based on the image operators mentioned herein (i.e. mean, variance etc). With a successful extraction algorithm, a CNN model of the object can be achieved.

3.1 Defining a Multiple Object Scene

Consider the problem of learning about one object which can appear at various locations in an image. The object is in the foreground, with a background behind it. This

background can either be fixed for all training images, or vary from image to image. The two key issues that must be dealt with are pixels being modeled as foreground or background, and the problem of transformations of the object [26][27]. A multi-object scene may be very difficult to model as the background may cause pixel infringements with the objects, and the objects themselves may cause pixel continuity with one another such that the edges are not detectable. It is also important to note that a background can be any feature that is of no interest in the main scene. This introduces an interesting notion that complicates this problem further, which allows the background to vary on a single scene. A human eye is capable of performing detection and segmentation of the object in varying background scenes. For comparison purpose, the algorithm used in modeling and detecting images on a multiple object scene in this case must have the ability to deal with background changes as in the human eye. Thus to approximate this, a method that operates on individual image pixels than one that assumes average pixel intensities over the image area is required. For this reason Cellular Neural Networks are chosen due to their ability to map each processing unit of the network to a pixel in the image. In Figure 3.1, a multiple object scene with objects in a black background is shown, while in Figure 3.2 a different scene wherein an object is defined as a feature of interest and any other feature that is not being studied is treated as a background.

Figure 3.1: An example of a multiple object scene using objects spatially distributed in the foreground of the image

Figure 3.2: An example of a multiple object scene with features/objects where the background depends on the feature/objects of interest [28]

3.2 Image Preparation

Image-capturing devices and surrounding environment may lead to corruption of the image with additive Gaussian, in which case the filters are required for noise reduction and image enhancement [29]. There are techniques available for designing these filters using CNN architecture.

The mean image is computed through linear diffusion applied to a coupled AB-type CNN network [31-33][41-44]. Equations 3.1 and 3.2 represent the AB-type CNN model and the diffusion type template that is used to derive the mean image in the CNN model, respectively.

$$\dot{x} = -x + \sum A(ij;kl)y_{kl} + \sum B(ij;kl)u_{kl} + I_{ij} \tag{3.1}$$

$$A = \begin{pmatrix} a & b & a \\ b & 0 & b \\ a & b & a \end{pmatrix}, \quad B = \begin{pmatrix} a & b & a \\ b & 0 & b \\ a & b & a \end{pmatrix} \tag{3.2}$$

where $0 \leq a, b \leq 1$

The variance of the image in the CNN domain is computed through the average difference method implemented as a nonlinear B-type template or the Laplace [32]. The network of this type is as represented in equation 3.3.

$$\dot{x}_{ij} = -x_{ij} + \sum B(ij;kl)(\Delta u_{kl}) + \sum \hat{B}(ij;kl)(\Delta u_{kl}) + I_{ij} \tag{3.3}$$

where $\hat{B}$ is the nonlinear input control template.
The CNN template associated with the architecture defined by equation 3.3 is shown in equation 3.2.

$$B_b = \frac{1}{n}\begin{pmatrix} 1 & 1 & 1 \\ 1 & 0 & 1 \\ 1 & 1 & 1 \end{pmatrix},$$

$$b = [interp \quad pnum \quad x_1y_1,\ x_2y_2\ \ldots\ x_ny_n] \tag{3.4}$$

where $A = 0$, $\hat{A} = 0$, $n \epsilon \Re > 1$ is the scaling factor, *interp* is the interpolation method (i.e. piecewise constant or piecewise linear), *pnum* is the number of points and $x_1y_1 \ldots x_ny_n$ are the interpolation points.

Figures 3.3 and 3.4 show the results of mean an variance of the image using the templates discussed above for $a = 0.1$, $b = 0.15$ and $n = 16$.

3.3 CNN Image Processors

3.3.1 Constrained Diffusion

Partial Differential Equations (PDEs) based methods have been used in the past to perform a variety of image processing tasks such as smoothing and restoration. The simplest and easily achievable PDE method for these tasks is the linear diffusion [33]

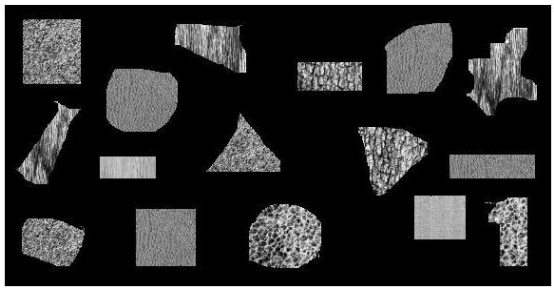

Figure 3.3: An image scene with multiple texture objects

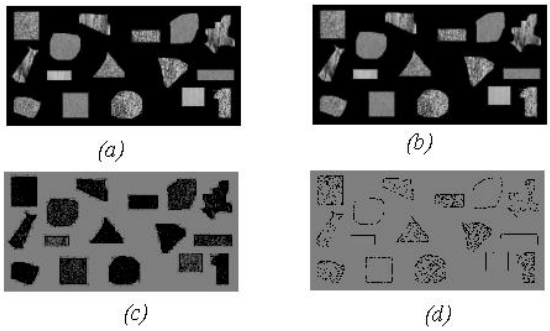

Figure 3.4: The mean and variance results computed using the space distributed templates in equations 3.2 and 3.2. (a) and (b) show the mean images at $\lambda = 0.3$ and $\lambda = 0.7$ respectively, and (c) and (d) show variance images using average difference and nonlinear deferential equation methods

model. However, PDE-based methods for edge detection and segmentation are computationally intensive and often present implementation difficulties [29]. A solution to this came with the introduction of a nonlinear diffusion method for adaptive smoothing by Perona and Malik [34], called Constrained Diffusion. Through constrained diffusion, the image is (1) smoothed using linear diffusion, and (2) the pixels are clipped so that the variation is within a desired threshold through a non-linear constraint step [35]. The realisation of the nonlinear constraint is a result of further research on the initial proposal by Perona and Malik, which led to the development of a "variational regularization method for global edge detection"[29], termed *Constrained Anisotropic*

Diffusion [36-38]. A CNN model representing this type of diffusion method is defined by the following set of equations.

$$\hat{D} = \begin{pmatrix} 0 & \Phi & 0 \\ \Phi & 0 & \Phi \\ 0 & \Phi & 0 \end{pmatrix}, \quad \Phi = g\Delta v_{xx}$$

$$g = \begin{cases} 1 - |\Delta v_{xx}|/2K & if\ |\Delta v_{xx}| < 2K \\ 0 & otherwise \end{cases}, \quad B = \beta(.)(3.5)$$

There are two ways in which anisotropic diffusion can be realised in the CNN domain. These are dependent on the type of constraint that is adopted (i.e. linear or non-linear constraint). The following methods are used for the design of linearly and nonlinearly constrained anisotropic diffusion [30].

(i). Nonlinear, Linearly Constrained Anisotropic Diffusion

This type of nonlinear diffusion employs the use of a linear constraint. This is done by performing *pixel intensity averaging* through a B-type template and scaling the B-template using a linear constraint. The constraint is chosen by the implementer. The output of the average difference network is then used as a bias to a nonlinear D-type diffusion template [30]. This is demonstrated through the following steps:

Step 1: Pixel intensity averaging through a B-type template.

$$A = 0, \quad B = \frac{1}{n}\begin{pmatrix} 1 & 1 & 1 \\ 1 & 0 & 1 \\ 1 & 1 & 1 \end{pmatrix} \tag{3.6}$$

where n is the scaling factor for linear diffusion.

Step 2: Scaling the B-template using the constraint and applying the average intensity

image computed in Step 1 as a bias to perform a nonlinear diffusion.

$$B = \frac{1}{4 \times constr} \begin{pmatrix} \frac{constr}{4} & \frac{constr}{2} & \frac{constr}{4} \\ \frac{constr}{2} & constr & \frac{constr}{2} \\ \frac{constr}{4} & \frac{constr}{2} & \frac{constr}{4} \end{pmatrix} \tag{3.7}$$

where *constr* is a constant linear constraint.
Using the output of *Step 1* and the template B resulting from the constraint, the nonlinear diffusion is computed using the nonlinear D-type template.

$$anisoD = \begin{pmatrix} 0.5 & 1.0 & 0.5 \\ 1.0 & 0.0 & 1.0 \\ 0.5 & 1.0 & 0.5 \end{pmatrix}$$

$$anisod = [interp \;\; pnum \quad p_{x1}p_{y1}, \quad p_{x2}, p_{y2} \ldots p_{xn}, p_{yn} \quad intspec] \tag{3.8}$$

where $p_{x1}, p_{y1} \ldots p_{xn}, p_{yn}$ are interpolation coordinates and *intspec* is the interaction specification [30].
The diagram in Figure 3.5 shows the flow associated with this analogic algorithm.

(ii). Nonlinear, nonlinearly Constrained Anisotropic Diffusion

This method employs a nonlinear constraint. In this algorithm, the median image is computed using the uncoupled nonlinear D-type template with $a_{00} = 1$. The constraint here is determined by the bias current I of the network. The median image is then used as a bias image to compute nonlinear diffusion using the same equation as in equation 3.8[30][41-44]. The following are the necessary steps required to achieve this algorithm:

Step 1: Median Filtering through uncoupled nonlinear D-type template.

$$a_{00} = \begin{pmatrix} 0 & 0 & 0 \\ 0 & 1 & 0 \\ 0 & 0 & 0 \end{pmatrix}, \quad Dd = \frac{1}{n} \begin{pmatrix} 1 & 1 & 1 \\ 1 & 0 & 1 \\ 1 & 1 & 1 \end{pmatrix},$$

$$d = [interp \;\; pnum \quad (p_{x1}, p_{y1}) \; (p_{x2}, p_{y2}) \quad intspec],$$

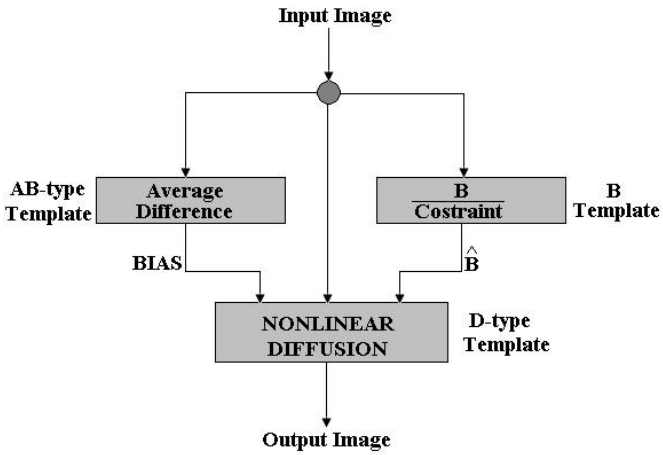

Figure 3.5: Flow diagram representing the nonlinear, linearly constrained anisotropic diffusion

$$I = constr \tag{3.9}$$

where $0 > n > 1$.

Step 2: Using the median image acquired in *Step 1* as a bias image to compute the nonlinearly constrained and diffused image. The nonlinear diffusion used here is the same as one represented in equation 3.8. The diagram in Figure 3.6 shows the flow associated with this analogic algorithm.

3.3.2 Adaptive Thresholding

Adaptive thresholding is one of the most essential steps in image detection. Thresholding determines which pixel intensities in a scene represent the characteristic patterns that can be separated in subsequent steps simply by thresholding the image enhanced using one of the procedures discussed in section 3.3.1. In simple terms, thresholding means driving all pixels to black that are above a given threshold value ϑ while leaving all others white or vice versa [39]. It is also known from Chapter 2 that the amount of current on the CNN network is controlled by the voltage controlled current source I. In analogy to this, the pixel intensity in the CNN model of the image is controlled by the

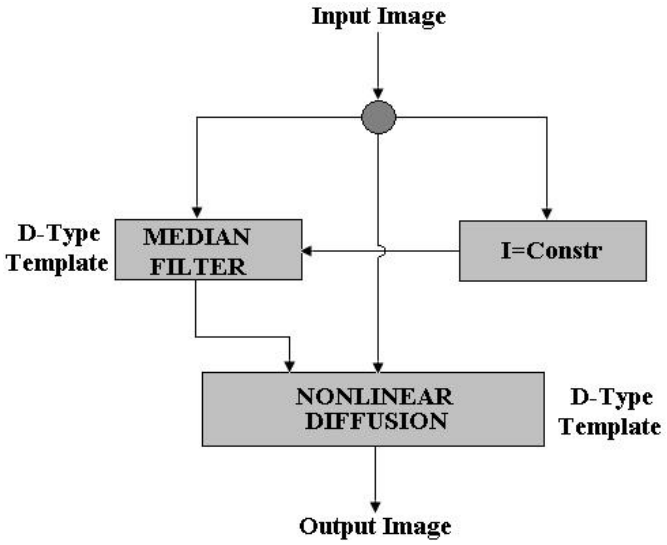

Figure 3.6: Flow diagram representing the nonlinear, nonlinearly constrained anisotropic diffusion

CNN bias current I. Thus, we set the bias current as the threshold. CNN-based adaptive thresholding is performed using both static and dynamic locally adaptive thresholding methods. The following defines each of these procedures and show how they are implemented into CNN templates:

(a). For static adaptive thresholding, we scale the input control template B of the CNN network appropriately in accordance with the threshold ϑ set for the application. In achieving this we make use of an AB-type CNN [30][41-44].

$$A = \begin{pmatrix} 0 & 0 & 0 \\ 0 & 3 & 0 \\ 0 & 0 & 0 \end{pmatrix}, \quad B = \frac{1}{(4 \times \vartheta)} \begin{pmatrix} \frac{\vartheta}{4} & \frac{\vartheta}{2} & \frac{\vartheta}{4} \\ \frac{\vartheta}{2} & \frac{\vartheta}{4} & \frac{\vartheta}{2} \\ \frac{\vartheta}{4} & \frac{\vartheta}{2} & \frac{\vartheta}{4} \end{pmatrix}, \quad I = -\vartheta \tag{3.10}$$

where ϑ is the constant threshold set for the application.

(b). For dynamic adaptive thresholding, the following AB-template is used.

$$A = \begin{pmatrix} 0 & a & 0 \\ a & 2a & a \\ 0 & a & 0 \end{pmatrix}, \quad B = \begin{pmatrix} \frac{1}{2\alpha} & \alpha & \frac{1}{2\alpha} \\ \alpha & 4\alpha & \alpha \\ \frac{1}{2\alpha} & \alpha & \frac{1}{2\alpha} \end{pmatrix}, \quad I = -\vartheta \tag{3.11}$$

where $0 \geq a \geq 1$, $0 \geq \alpha \geq 1$ and ϑ is the constraint.

This technique is based on the adaptive morphology technique that is proposed by Rekeczky *et al* [29] as an approach to Bubble/Debris image enhancement.

3.3.3 CNN-based Object Detection, Segmentation and Extraction Strategies

Object detection result as a consequence of a better threshold that suppresses the background into black or white pixels. A success in the thresholding method yields better results when an object has to be defined as a set of connected pixels of intensities above a certain threshold. The segmentation technique visits the original or enhanced image scene to locate the pixels that represent the objects. The representation of the segmented objects rely on the nature of the thresholding used above. There is a variety of methods for implementing CNN-based edge detection and segmentation. In this case two methods, namely linear and nonlinear template based methods will be explored.

1. (a). Linear Edge Detector - Since a CNN model is already nonlinear, what is linear about this type of detector is the cloning template that describes the behaviour of the network. The implementation of this type of detector is achieved through the use of the uncoupled AB-type templates. By decoupling each pixel from the neighbouring pixels, its influence in the network is studied in isolation. This allows for the method to determine whether the pixel forms the object or the object edge accordingly with the required threshold. The templates of this type are represented by the set of matrices in equation 3.12.

$$A = \begin{pmatrix} 0 & 0 & 0 \\ 0 & 2a & 0 \\ 0 & 0 & 0 \end{pmatrix}, \quad B = \begin{pmatrix} \frac{1}{4a} & \frac{1}{4a} & \frac{1}{4a} \\ \frac{1}{4a} & 2a & \frac{1}{4a} \\ \frac{1}{4a} & \frac{1}{4a} & \frac{1}{4a} \end{pmatrix}, \quad I = -\frac{3}{4a} \tag{3.12}$$

where a is normally chosen to be greater than 1.

2. (b). Nonlinear Edge Detector - This detector is based on a nonlinear AB-type network [30][41-44]. This detection technique yields enhanced edges of the object through further image smoothing. It inherits this behaviour from the nonlinear diffusion techniques discussed in section 3.3.1, which are used for image filtering and enhancement. In this case a nonlinear B-type input control template is applied to an object as shown in equation 2.

$$Bb = \begin{pmatrix} a & a & a \\ a & 0 & a \\ a & a & a \end{pmatrix},$$

$$b = [interp \;\; pnum \quad (x_1, y_1),\ (x_2, y_2) \ldots \quad intspec] \tag{3.13}$$

where $0 \geq a \geq 1$

With all object edges detected, an extraction of the object based on the permutations of the edges is performed. For the purpose of simplicity, it will be assumed that that all the objects in the multi-object scene do not have holes. This allows for implementation of hole filling for holes that appear inside the trace of an object edge. The extraction is done on the original CNN enhanced image.

3.4 The Analogic Algorithm for Object Extraction in Multiple Object Scenarios

In this section, the algorithm proposed to handle multiple object extraction is presented. This algorithm is formulated as a combination of the CNN image processors discussed in section 3.3. The design of this algorithm is also inspired by the algorithm proposed in [29]. This algorithm is extended to perform extraction of enhanced objects for the purpose of learning and classification. It is based on constrained anisotropic diffusion with adaptive local thresholding and 8-connected edge detection.

3.4.1 The Proposed Algorithm

The algorithm involves computing the mean and variance of the image to get a bias map to be used for adaptive thresholding, this technique was adopted from [29]. The object is smoothed and enhanced using constrained anisotropic diffusion. While the superposition of mean and variance yields a bias map for adaptive thresholding, the output of the constrained anisotropic diffusion is used as an input image for this stage. The output of the adaptive thresholding is used to perform segmentation. From the output of the edge detector, all permutations of the object edges are extracted through boundary tracing and hole filling. By mapping the traced boundaries and the permutations onto the CNN enhanced image of the original scene, all pixels within the boundaries forming the object are extracted. Figure 3.7 shows the flow of the proposed algorithm.

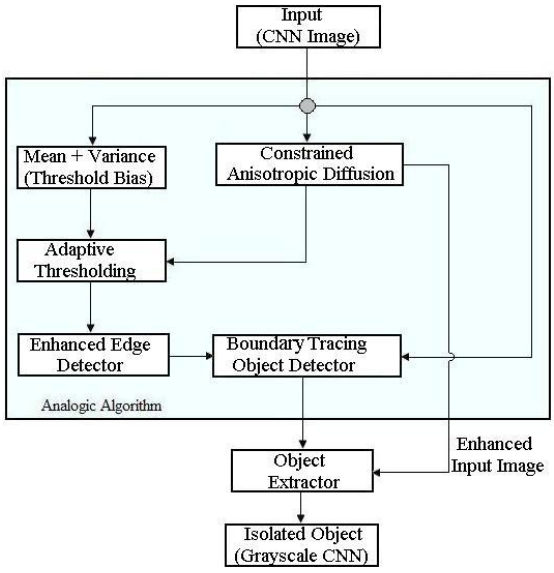

Figure 3.7: Proposed extraction algorithm: Constrained anisotropic diffusion with adaptive thresholding

3.4.2 A Practical Example

This section demonstrates the extraction ability of the algorithm herein proposed through an example. The example is a scene with multiple coins of different sizes and prints

as shown in Figure 3.1. The extraction algorithm is applied to the scene to extract all objects appearing in it such that each object is viewed in isolation. The results are as shown in Figure 3.8. The objects are shown in the order of appearance in the input image. The efficiency and accuracy of extraction of the objects from the scene has a profound impact on the CNN model of the objects. If the extraction algorithm cannot successfully extract the object, the learning of object features is hampered.

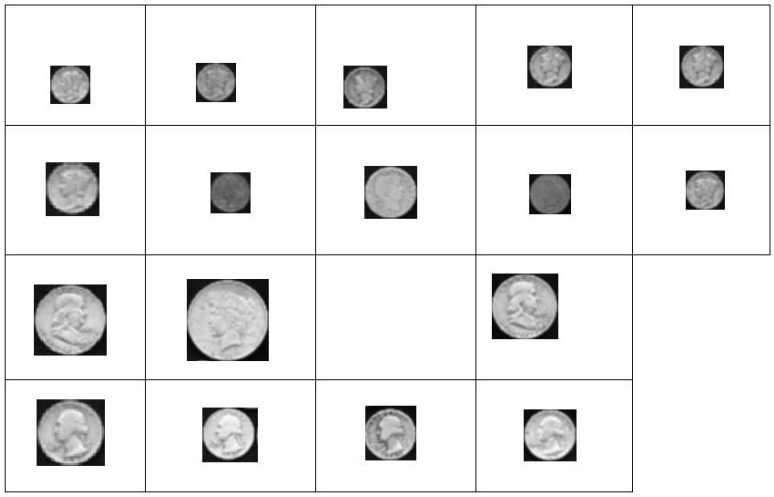

Figure 3.8: Objects Extracted using the proposed extraction algorithm

Chapter 4

Feature Selection and Extraction Strategies for CNN Classification Models

The performance of a classification method relies on the art of gathering the most unique attributes of the learned object. This art can be derived from both mathematical and analytical methods. In this chapter, some feature extraction strategies are formulated based on existing theories. Some existing methods will be adopted based on their performance in the field of multiple object learning and classification. The methodologies for gathering, analysing and manipulating object features to create decision boundaries are also formulated. This chapter will first outline the strategies used to create decision boundaries and then further introduces methods of extracting features such as texture, shape and colour with reference to the storage and representation in the CNN domain.

4.1 Signature Filtering and Decision Boundaries

Features gathered from different objects representing one class must be checked for consistency and uniqueness [23]. This is to avoid listing features that are only local to an object as global features representing a class. The procedure formulated in [23] involves defining threshold values for an acceptable standard deviation and mean between two

signatures. For a signature to be unique in a class, it must have a standard deviation and mean unique to the class. This ensures that all signatures containing the same features as those already learned are ignored. Thus,
Scaling all signatures belonging to a class, we use

$$stddev(X_{sb}) < thres_1 mean(X_{sb}) \tag{4.1}$$

where X_{sb} represent the measured signature X_s belonging to class b.

For each class, ensure that the mean for each specific measurement varies within a defined range. This means that any measurement X_s of with a mean outside the threshold range of a class does not belong to that particular class.

$$Mean(X_{sc}) - Mean(\hat{X}_{sc}) < thres_2 \tag{4.2}$$

where $\hat{X}_{sc}$ is a new measurement belonging to class c.

In [23] a strategy for feature selection for supervised learning algorithms is also presented. This is done by predefining the required classes and capturing the most distinctive features for each class. A strict discrimination of features in the classes is designed to avoid conflicts. Thus,

$$\underset{s}{^{arg}\ ^{max}} |(mean(X_{sa}) - mean(X_{sb})| > thres_3 \tag{4.3}$$

and for signatures belonging to one class a:

$$\underset{s}{^{arg}\ ^{max}} |(mean(X_{sa}) - mean(\hat{X}_{sa})| > thres_4 \tag{4.4}$$

where $\hat{X}_{sa}$ is a new measurement belonging to class a.

These techniques have been adopted and modified to suit this application. Of great importance is the procedure of storing this information [47]. For complex processing the patterns or signatures must be stored in the CNN network itself. We explore how features can be stored as stable memories in the CNN architecture.

4.2 Texture Measurement Methods

Texture is a description of the spatial arrangement of color or intensities in an image or a selected region of an image [48]. While edges and image lines are visual aspects of the image, texture is the statistical measure of intensity distribution in the image. The most common aspects of textures that are normally encountered are size or granularity (e.g. sand versus pebbles versus boulders), directionality (e.g. stripes versus sand), random or regular (e.g. sawdust versus woodgrain; stucko versus bricks) and spatial arrangement of texels [48]. The process of segmenting texels in real images is quite difficult. As a result, numeric quantities or statistics that describe a texture are used. Several measures of texture are described below:

(i) First Order Measures - These techniques measure the edge density and direction of the texels in one texture. The number of pixels representing the texture in one specific area carries information about how busy that area is [48]. The characterization of the texture in that specific area is done by computing the direction of the edges. This procedure follows the steps below:
Step 1. Compute the edgeness of the texture per unit area.

$$\frac{\left\{p|gradient_{mag}(p) \geq threshold|\right\}}{A}$$

where p is a pixel forming a texel and A is the unit area.

Step 2. Compute Magnitude and Directions histograms and develop heuristic for measurements.

$$Hist = (Hist_{mag}, Hist_{dir})$$

where $Hist_{mag}$ and $Hist_{dir}$ are magnitude and direction histograms, respectively.

(ii) Statistical Measures - This is the best model for most natural textures [48]. Statistical filters are used to measure the first order grey level metrics of a texture based on histograms. Gabor filters [49] are then used to get a strong response (frequency) at points in an image where there are components that locally have a particular spatial frequency and orientation.

4.2.1 CNN Template Design for Texture Analysis

In chapter 2, it was shown that the behaviour of a CNN is influenced by the convolution kernels A, B and I which are commonly referred to as the Cloning Templates. For a CNN network to successfully extract features and store them for a later recall, the Cloning Templates must capture the features of the object, which include texture. There are various CNN templates that can be used to achieve this, but the simplest and to implement is the linear AB-type template. For most spatio-temporal processes, the templates are required to be space invariant. In [41], a template that can be used in a texture classification problem when the number of different examined textures is, for instance, more than 10 and the input textures have the same flat grayscale histograms is designed. The template parameters are set as shown in equation 4.5:

$$A = \begin{pmatrix} 4.21 & -1.56 & 1.56 & 3.36 & 0.62 \\ -2.89 & 4.53 & -0.23 & 3.12 & -2.89 \\ 2.65 & 2.18 & -4.68 & -3.43 & -2.81 \\ 3.98 & 1.56 & -1.17 & -3.12 & -3.20 \\ -3.75 & -2.18 & 3.28 & 2.19 & -0.62 \end{pmatrix},$$

$$B = \begin{pmatrix} 4.06 & -5 & 0.39 & 2.11 & -1.87 \\ 3.90 & 0.31 & -1.95 & 4.84 & -0.31 \\ 0 & -4.06 & 0.93 & -0.31 & 0.46 \\ -0.62 & -5 & 2.34 & 0.62 & -1.87 \\ 3.59 & -0.93 & 0.15 & 2.81 & -1.87 \end{pmatrix}, \quad z = -5 \tag{4.5}$$

As highlighted above, this template is only suitable for a certain class of textures. The templates remain fixed for any data input, thus suggesting that the method is not adaptive and hence cannot be conveniently used for general classification purposes. We explore other methods of designing adaptive cellular neural networks that can be used to capture spatio-temporal properties of objects.

4.2.2 Histogram Based Texture Learning Methods

Histograms store important information about the texels in the object [48]. This information is normally represented by the amplitudes of the histogram or the distribution.

By performing further histogram modification and diffusion filtering, more distinctive image features can be learned [53][54]. A drawback in this approach is a lack of a better method to compare histograms. There are several heuristics that can be use to compare histograms. One is to determine the highest intensity amplitude in the histogram and the number of bins with such intensity in the object. The idea here is that all textures that exhibit the same behavior or pattern will have the same amplitudes centered around the same number of bins per intensity. This idea is demonstrated below through some texture examples. Consider 3 classes of textures shown in the Figures 4.1 to 4.7. For demonstration purposes, we will call the textures Class 1, Class 2 and Class 3 respectively.

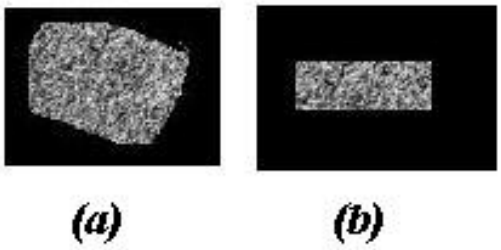

Figure 4.1: Class 1 Texture: (a) and (b) are two texture objects used to learn the histogram behaviour of Class 1 textures. Edited from the columbia image database [54]

Analysis

From figure 4.10, it is possible to create the decision boundaries based on the modified and diffusion filtered histogram features in each of the classes. Each texture class exhibit a specific and unique order of the magnitudes of the pixel intensities. The distribution of the intensities is also a distinctive factor. Class 1 textures have their highest intensity magnitudes centered just above 200 bins, while Class 2 textures have their highest magnitudes below 100 bins. While Class 2 only have one intensity magnitude centred below 100 bins, Class 1 textures have two magnitudes centred just after 100 and 150 bins respectively. Class 3 textures have two intensity magnitudes centered at just above 100 and 200 bins respectively with a relationship that can be generally described

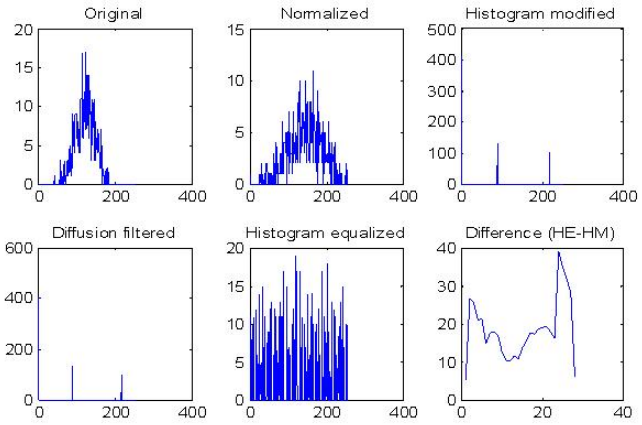

Figure 4.2: Histograms Associated with Class 1 Object (a) textures

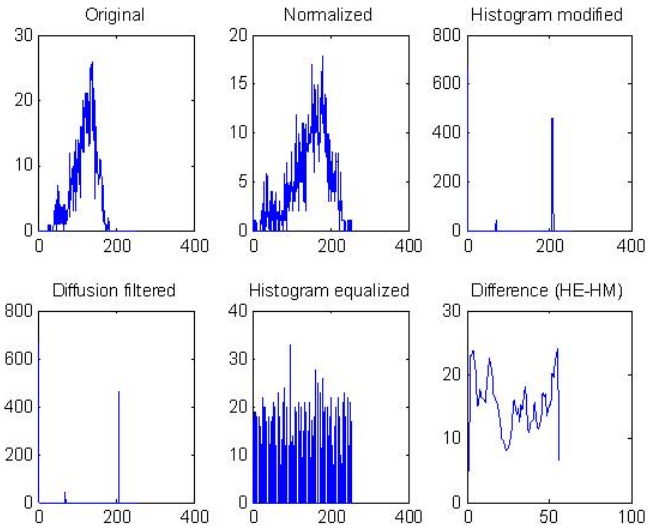

Figure 4.3: Histograms Associated with Class 1 Object (b) textures

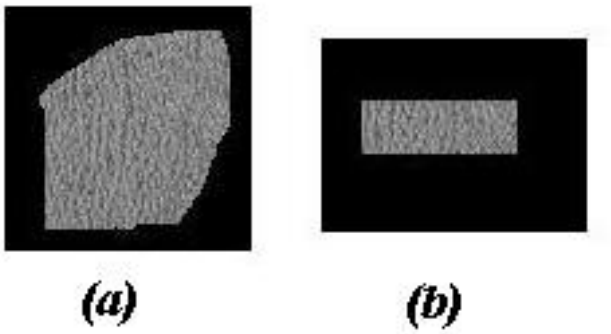

Figure 4.4: Class 2 Texture: (a) and (b) are two texture objects used to learn the histogram behaviour of Class 2 textures. Edited from the columbia image database [54]

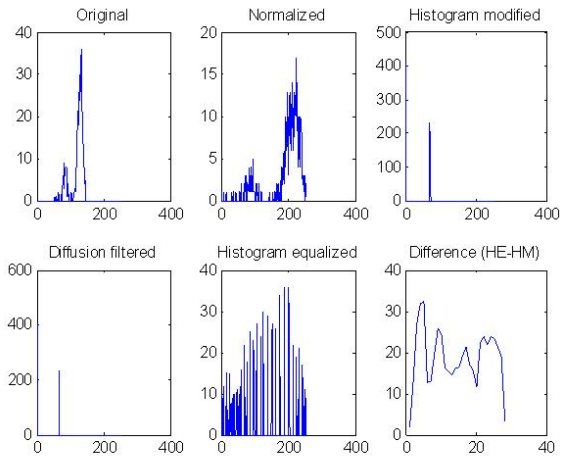

Figure 4.5: Histograms Associated with Class 2 Object (a) textures

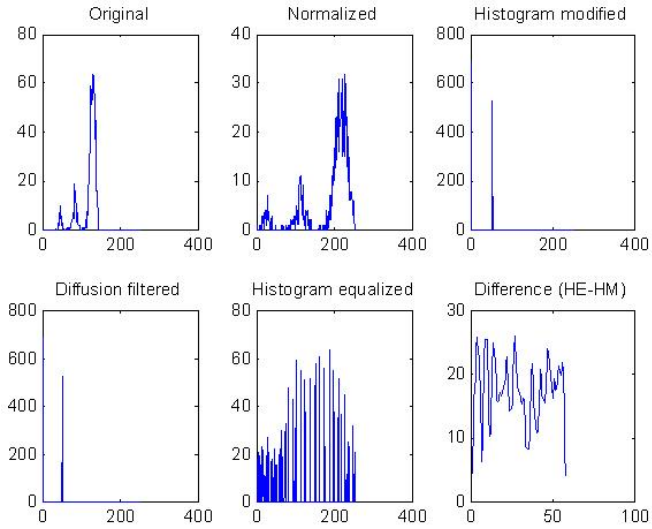

Figure 4.6: Histograms Associated with Class 2 Object (b) textures

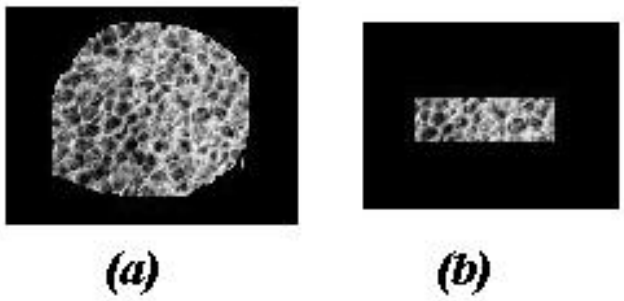

Figure 4.7: Class 3 Texture: (a) and (b) are two texture objects used to learn the histogram behaviour of Class 3 textures. Edited from the columbia image database [54]

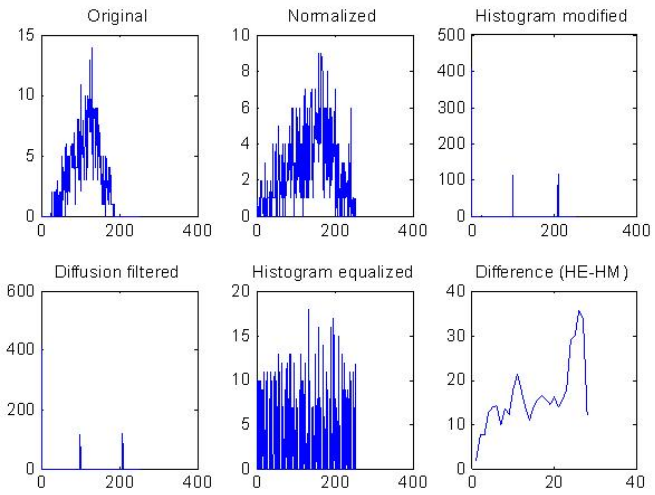

Figure 4.8: Histograms Associated with Class 3 Object (a) textures

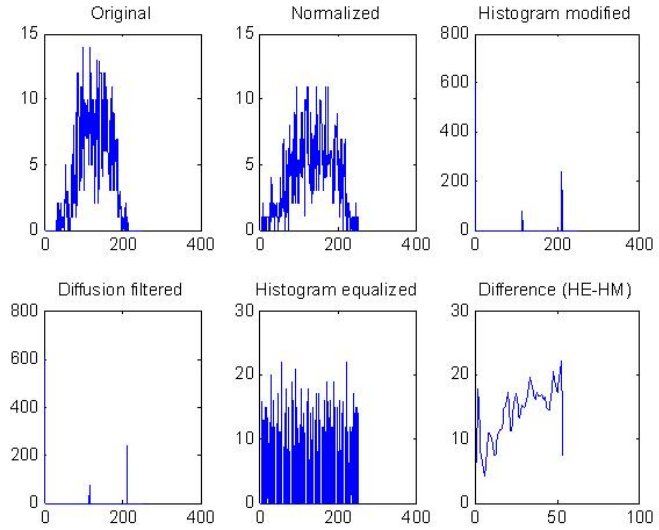

Figure 4.9: Histograms Associated with Class 3 Object (b) textures

by $I_{100+} \geq \frac{3}{2} I_{200+}$. Based on these results, the following boundary rules can be designed for each class. We first define I_{max1} and I_{max2} as the first and the second highest texel intensities measured through the histogram modification of the texture histograms.

Class 1 Textures:

-I_{max1} is located at $p > 200$

-I_{max2} is located at $p < 100$

-$|I_{max2}| < |\frac{1}{2} I_{max1}$

Class 2 Textures:

-I_{max1} is located at $p < 100$

-I_{max2} is located at $p < 100$ or $I_{max2} = 0$

-For $I_{max2} \neq 0 :\ |I_{max2}| \geq |\frac{1}{2} I_{max1}|$

Class 3 Textures:

-I_{max1} is located at $p > 200$

-I_{max2} is located at $p > 100$

-$|I_{max2} \geq \frac{3}{4} I_{max1}$

These decision rules can be implemented into an algorithm that can be used to classify textures into the 3 classes defined here. The underlying drawback in using this method is that it is manual and nonadaptive. When a new class of texture needs to be created, the decision boundaries have to be setup manually. Also, the texture pattern may be too complicated for one to set up operating conditions that best describes that texture. An ideal method for this should be adaptive and easy to train. The algorithm for designing the decision rules should be embedded in the method itself. For this reason, in section 4.4 we propose a new method that best suits this application.

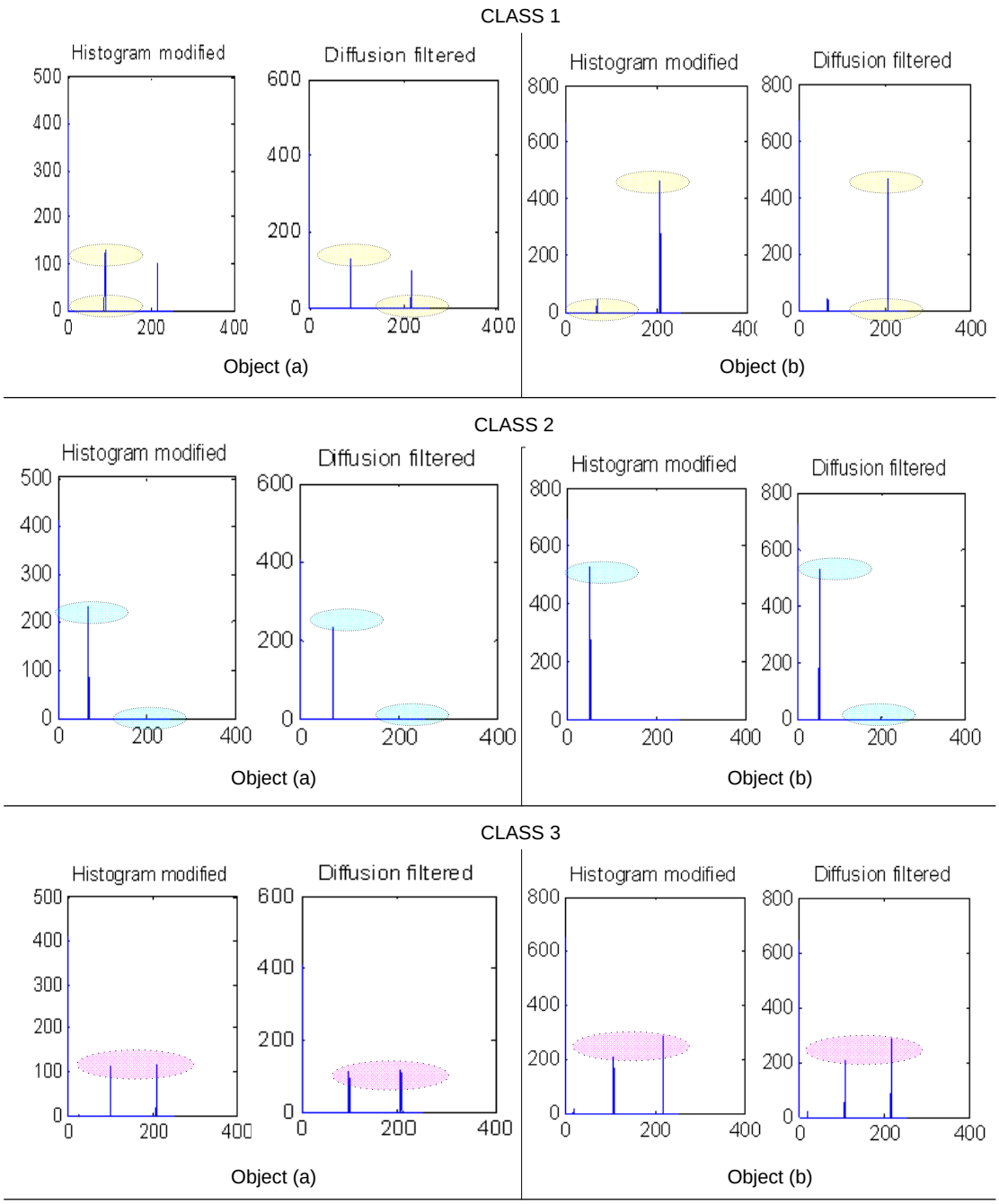

Figure 4.10: Comparison Diagram for Modified and Diffusion filtered histograms for the 3 texture classes. The shaded circles indicate unique features captured through these types of histograms

4.3 Template Synthesis Procedures For Learning Object Features

In the design of associative memories for learning the spatio-temporal properties of objects, one has to take into account that the template values are the main feature database of a class. Template design can be very complex as all template values have to be calculated or estimated to result in the required coupling between the cells. The templates have to store the most significant features of the object. Liu and Lu [15] have designed a procedure through which a space invariant template can be synthesised. They apply the eigenstructure method in which the nonlinear CNN equations are solved by singular value decomposition procedure to manipulate the template parameters. The algorithm is based on the uncoupled associative network represented by the set of equations in 4.6.

$$\dot{x}_{ij} = -a_{00}x_{ij} + \sum T(ij,kl)y_{ij} + I_{ij}$$
$$y_{ij} = sat(x_{ij}) \tag{4.6}$$

The challenge is to design the feedback cloning template $T(ij,kj)$ such that it properly represents the stable memories of the feature vectors learned for the object. This procedure is summarized as follows [15, 50-52]:

1. Choose Vectors β^i for $i = 1,\ldots,n$ and a diagonal matrix A such that:
$A = diag(a_1, a_2, \ldots, a_i)$ and,
$A\beta^i = \mu\alpha^i$ where α^i are stable memories and μ is a constant ($\mu \geq max(a)$)
2. We compute the $nx(m-1)$ matrix $Y = (y^1,\ldots,y^{m-1}) = (\alpha^1,\ldots,\alpha^{m-1},\alpha^m)$
3. The next step is to use singular value decomposition to solve the matrices $Y = USVT^T$, where U and V are unitary matrices and S is a diagonal matrix with the singular values of Y on its diagonal.
4. Compute
$T^+ = [T^+_{ij}] = \sum i(u^i)(u^i)^T$ for $i = 0,\ldots,p$, and
$T^- = [T^-_{ij}] = \sum i(u^i)(u^i)^T$ for $i = p+1,\ldots,n$
5. Choose a positive value for parameter τ and compute

$T = \mu T^{+} + \tau T+$ and $I = \mu\alpha^{m} - T\alpha^{m}$

6. Then $\alpha^{1}, ..., \alpha^{m}$ will be stored as memory vectors in the system 4.6.

This procedure yields a template $T(ij, kl)$ which is symmetric and stable [15].

4.4 Feature Selection and Learning using Genetically Optimized CNNs

In this method, we propose the use of genetic algorithms to create stable memories that store the features of the object. It is proposed that using the simplest CNN architecture, the template parameters that best captures the features of the input can be estimated through genetic algorithms. The method is based on optimising the parameters of the kernel matrix (or cloning template) of the associative network described in chapter 2. In practice, it may not be sufficient for the algorithm to be restricted into capturing certain input traits modeled as deterministic rules or mathematical equations. An algorithm that successfully selects the features without human intervention may yield better results as there is no mathematical restrictions to govern the selection procedure. The selection based on genetic algorithm tries to achieve this in practice.

4.4.1 Genetic Algorithms(GAs)

The main challenge that any optimization technique faces is termination at an optimal solution that describes the global behavior of a process. During optimization, a poor optimization method can get trapped in the local maxima, which may not be the best solution in the solution space. This problem is common to most linear optimization solutions.

Genetic Algorithms inherit their origins from the Darwinian theories of evolution [24,37,55-59]. In this theory, the survival of a gene is a result of natural selection through fitness. This natural process is achieved by applying certain genetic operators such as crossover and mutation. Through these operators new genes that adapt to the competition environment are created, therefore getting rid of unfit genes that do not optimize the solution.

Artificial GAs are based on stochastic sampling methods that increase the probability of

finding an optimal solution by creating somewhat controlled random searches through the entire solution space. The following describes the steps involved in these algorithms [58]:

BEGIN

1. Randomly create an initial population beginning at an initial generation. i.e. $P(g)$ @ $g = 0$.
2. for each population $P(g)$, evaluate each population member (chromosome) using the defined fitness evaluation function E possessing the knowledge of the competition environment.
3. using genetic operators such as inheritance, mutation and crossover, alter $P(g)$ to produce $P(g+1)$ from the fit chromosomes in $P(g)$.
4. repeat steps (2) and (3) for the maximum number of generations $G \geq g$, while recording the best population of all the generations.

END

An accurate model of the fitness function using mathematical formula that carries the knowledge of the competition environment is essential to the evaluation of the chromosomes. A poorly designed fitness test will sacrifice the accuracy in the selection and may lead to incorrect selection of genes. There is also a need to ensure that the system is stable . A bounded input result into a bounded output (i.e. BIBO stability), thus suggesting the need to control the bounds for all chromosomes that the GAs can generate.
GAs have been used to solve complex problems wherein the learning environment does not provide proper decision boundaries.

4.4.2 Integrating GAs into the CNN Architecture

The Zero-Input CNN (autoassociative) is chosen as the platform of computation for the spatio-temporal properties of the objects. The method proposed here is based on optimizing the feedback template to approximate the input U_{kl} that is supplied to the CNN as a state image. Using GAs, the output of a zero-input network is continuously

modified until it matches the state image. The GA uses the evaluation function E as a measure of how closely the input and the output images of the CNN are matched through the template $T(i, j; k, l)$ (derived from equation 4.6). The function E is the error between the input and the output image. Given:

$$\dot{X} = -X + \sum T(ij, kl)Y + I_{ij}$$

as the associative CNN network, the goal is to find the best $T(ij; kl)$ that captures the input traits and the bias I_{ij} required for the pixel intensities to be approximated. This concept is illustrated by the diagram in figure 4.11. Creating the next generation, $fitness = 1 - cost(T, I)$ is used to determine if the population has a high survival possibility. The fitness evaluation function is computed as the square error between the CNN output and the input training image. The square error is calculated to ensure that only the magnitudes of the errors are considered. This is shown in equation 4.7:

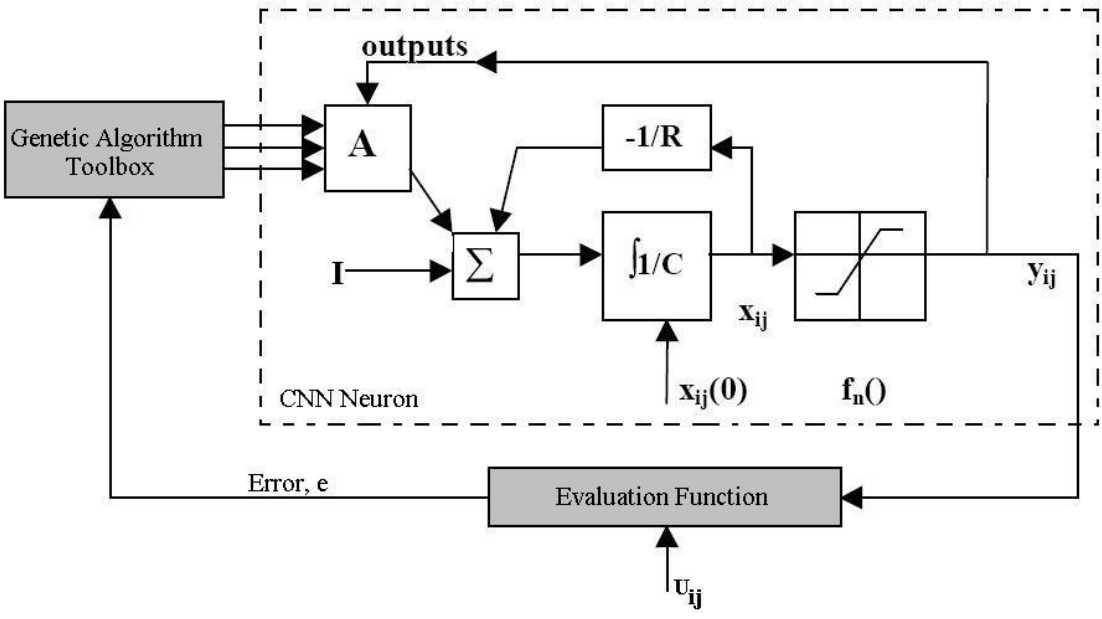

Figure 4.11: The Proposed CNN associative model based on GA optimization

$$E = -\sum (Y_{ij} - U_{ij})^2 \tag{4.7}$$

where Y_{ij} is the output of the CNN and U_{ij} is the training image (i.e. a small CNN image containing details about the feature(s) characterizing a class). GA evaluation technique is based on ensuring the highest value possible for the evaluation function (i.e. finding chromosomes that maximise E). However, in this case it is required that the smallest value possible be the optimal solution (i.e. reduced error). To ensure that GA minimizes the error, error equation is negated such that the maximum possible solution achievable in the network is zero.

With the CNN architecture adopted in this algorithm and a $3X3$ template, the total number of parameters that need to be stored is 10, 9 of which represent a 3 X 3 convolution kernel $T_{ij,kl}$ and one represents the CNN bias I_{ij}. It is well known that GA performance decreases when searching in large parameter space as it becomes computationally challenging to iterate through all elements and observing their contribution to the overall solution [38]. It thus becomes important to limit the number of parameters that require optimization. Also, it has been reported in [38] that a CNN based on a $3X3$ network has the ability to capture enough information on the training data.
The set of matrices in equation 4.8 represents a model of the chromosomes generated by GAs and used to create a CNN kernel [62]:

$$T(i,j;k,l) = \begin{pmatrix} seed(1) & seed(2) & seed(3) \\ seed(4) & seed(5) & seed(6) \\ seed(7) & seed(8) & seed(9) \end{pmatrix},$$

$$I_{ij} = seed(10) \tag{4.8}$$

The GA solution bounds for the elements in matrices $T_{ij,kl}$ and I_{ij} must be set in order to have result in a bounded output (i.e. bounds $[-x; +x]$ where $-x$ and $+x$ respectively denotes the lowest and the highest chromosome values expected in the generations).

Chapter 5

The Analogic Algorithms for Object Detection and Classification in Multiple Object Scenarios

This Chapter is the integration of all chapters that build up the basis of the proposed algorithms. In this chapter, both the learning and classification methods based on the discussions and propositions made in chapter 4 are developed. The main building blocks of the learning and classification algorithms proposed in this case are the object extraction from a multiple object scene, feature extraction and learning; and the classification of learned features into predefined classes. Two feature selection strategies for multiple object scenes are proposed, namely (1) feature learning through GA optimization and (2) texture learning through histograms.

The first method is based on designing autoassociative memories in the CNN model and optimizing feature learning using GAs. This is achieved through the use of a zero-input CNNs and genetically optimized, space-invariant cloning templates. For GAs to efficiently optimize the kernel matrices of the CNN, the number of kernel parameters

that require GA modification should be small. The choice of the autonomous CNN network facilitates the reduction of parameters in the kernel as the network only requires the feedback template and the bias current to be set up. With the choice of a $3X3$ network, the number of chromosomes required by the GA is reduced to 10.

The second approach that is proposed in this research is based on the comparisons of the diffusion filtered(DF) and modified(MD) histograms generated for each object texture. The shape and the locations of maximum intensities for different textures in the DF and MD histograms are different. This information is used to design decision boundaries for each texture class. A procedure for designing class boundaries by examining specific features in the histograms is proposed and outlined.

Firstly, this chapter introduces the spatio-temporal learning algorithm based on 3 stages, namely the preprocessing stage that removes gaussian noise and enhance the image, the object extraction technique that is based on boundary tracing and hole filling methods and the spatio-temporal learning of features in the object is done and the features therein are grouped into categories or classes. As these parts have already been discussed in the chapters above, the discussions in this chapter will mainly be centered on how they integrate to form a complete classification algorithm. Finally, the classification algorithm proposed for this application is outlined.

5.1 Classification Using CNN Associative Memories and GAs

5.1.1 The Extraction and Training Algorithms

An efficient algorithm for spatio-temporal learning is one that learns the most distinguishing features of the object from the environment in which the object appears in. If the object appears in a different environment alone, the algorithm should possess the knowledge to be able to detect the object. Taking this into account, the extraction of the object in order to learn it separately from the environment becomes the first step of the learning algorithm. The learning algorithm proposed here first implements

an analogic technique that filters out the noise and extract the object from a multiple object environment before learning takes place. This is an important step as objects in natural scenes do not often appear in the image alone. The extraction algorithm is based on anisotropic diffusion and adaptive thresholding discussed in section 3.3.1 and 3.3.2 respectively. The second part of the algorithm is training the CNN associative architecture for extraction and storage of input features as stable memories in cloning templates. The training is implemented as a recursive genetic learning approach that truncates the learning error towards an optimal solution (i.e globally stable memories). This algorithm is summerised by the flow diagram in figure 5.1. The learning algorithm can be described as follows:

1. For a $3X3$ network, start off with a gene population of 10 and generation 1. - estimate $T(ij, kl)$ and $I(ij)$ such that $Y = U$.

2. Evaluate the genes using the evaluation function $E = Y - U$ where Y is the output of the CNN and U is the training set. The smallest value of E indicates the similarity between the input and the output, and thus the optimal stable memories that must be stored in $T(ij, kl)$ and $I(ij)$

3. The process must be repeated for a number of n generations, while the genetic operators such as crossover and mutations are applied to yield the population for the next generation.

4. A class is a set of template parameters that represent learned features of objects with a similar behaviour (i.e. $T(ij, kl)$ and $I(ij)$ that are generated for each class).

Consider a multiple object image shown as an input of the learning algorithm in figure 5.2, the image is transformed for feature learning as shown by the optical flow in the processing stages of the proposed algorithm.

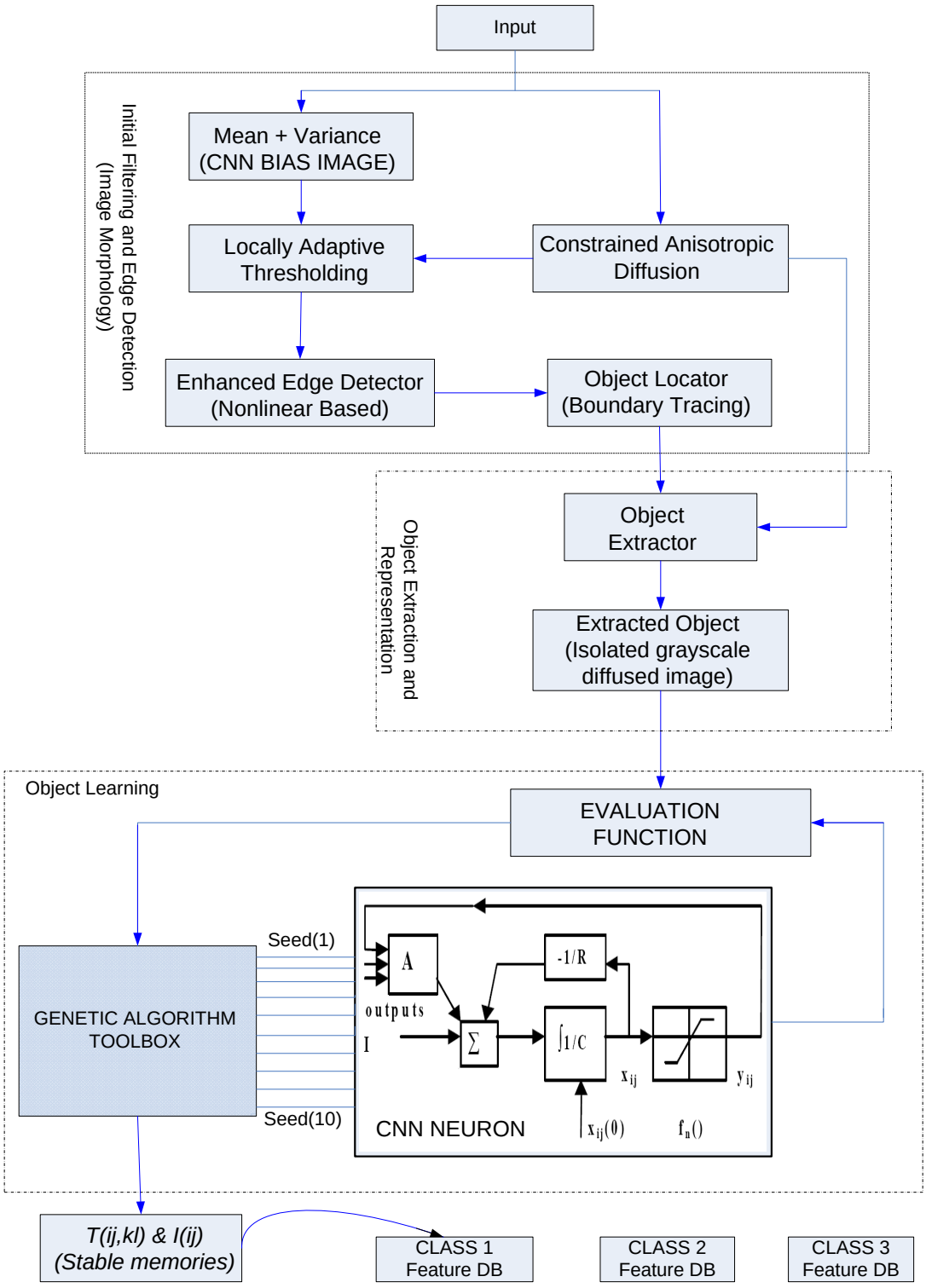

Figure 5.1: Proposed algorithm for learning spatio-temporal features of objects in multiple object scenes

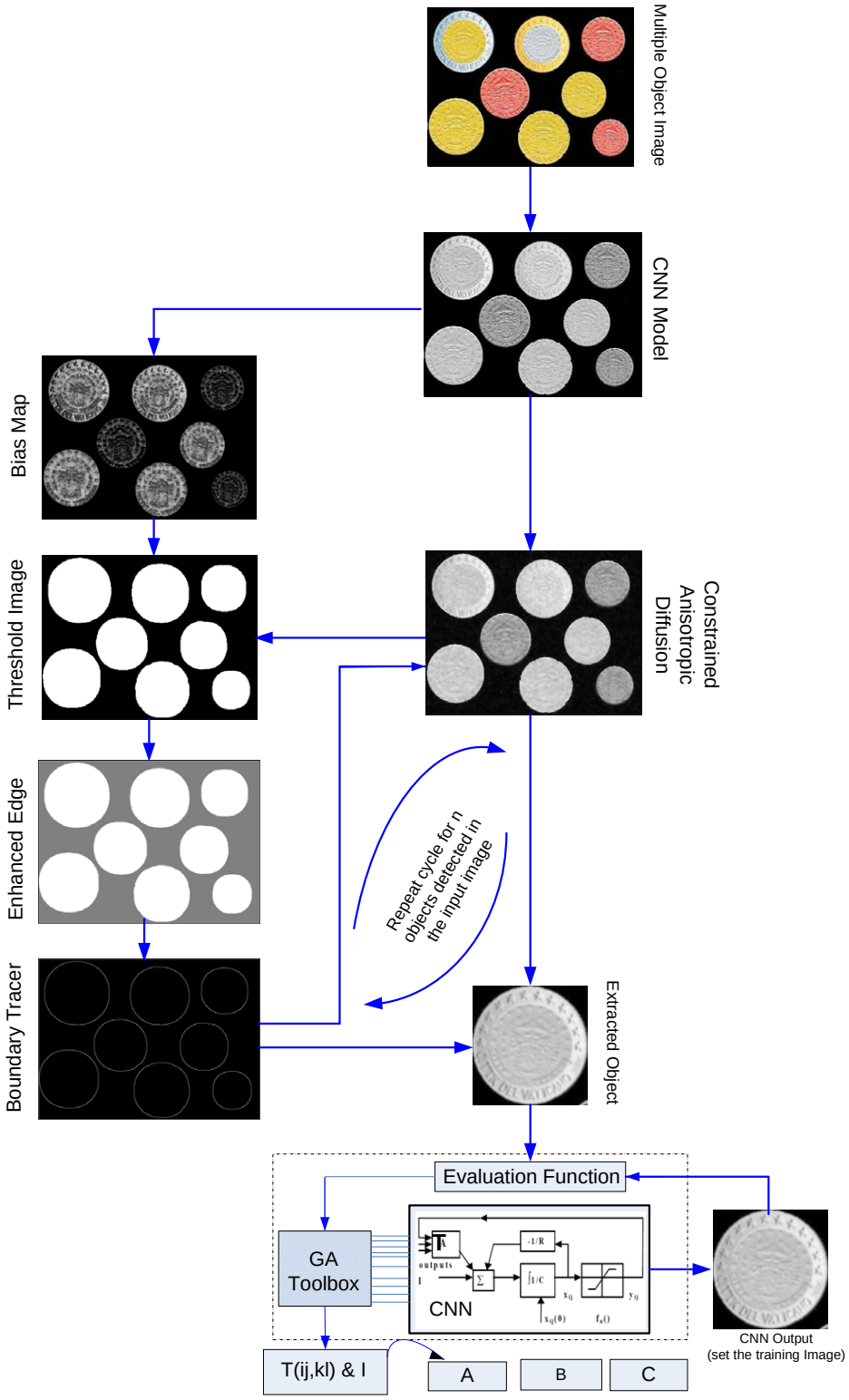

Figure 5.2: Optical flow of processing stages of the proposed algorithm

5.2 Texture-based Feature Extraction Using DF and MD Histograms

The concept of using histograms to perform classification tasks was outlined in section 4.2.2. Using diffusion filtered and modified histograms, different texel intensity magnitudes in the object are detected. The number of bins with the highest texel intensities in the histogram also represent how repetitive the texture pattern is. The number of non-zero intensity magnitudes represent the unevenness of that texture and the repetitiveness of each intensity. There are no established rules known in research for comparing different histograms. In this section, various heuristics are used to formulate a method for designing boundary conditions for each class based on the information captured in the DF and MD histograms.

Using the CNN model, the training objects are extracted from a scene and enhanced through CNN analogic algorithms for nonlinear diffusion and then MD and DF histograms are generated. The histograms for each of the textures are then compared to generate the decision boundaries that can be used to classify the textures. To generate the decision boundaries, three highest texel intensities and their respective number of bins are determined from the histograms and this information is compared for all objects in the same texture class. The bounds for the maximum intensities and number of bins per area A of a certain texture are determined and the information is then stored as class features.

Heuristics for Designing Texture-based Class Boundaries

From the illustrative DF histogram in Fig 5.3, we define:
-I_{max3}, I_{max1} and I_{max1} as the first, second and third highest intensities measured by the histogram for a particular texture object. $I_{max3} > I_{max2} > I_{max1}$
-*nbin* is the number of bins with a particular texel intensity in the image per predefined area A
-*pos* defines the bounds of an intensity magnitude in terms of number of bins
-$nomax2$ the boolean indicator for I_{max2} measurements

-$nomax1$ the boolean indicator for I_{max1} measurements
-n is a constant multiplier between texel intensities

-For A Class X texture shown in figure 5.3

- $I_{max2} > n * I_{max3}$. This condition determines the difference factor between the highest and second highest intensities in the texture image.
- For I_{max3}: $0.75 * nbin < pos < nbin$. The condition gives the bounds for number of bins with highest maximum intensities in area A.
- For I_{max2}: $0.5 * nbin < pos < 0.75 * nbin$. This condition is necessary to determine the bounds for number of bins with I_{max2} intensities
- If $I_{max2} == 0 : nomax2 = 0$ else $nomax2 = 1$. This condition is necessary for textures with only 1 non-zero intensity magnitudes.
- If $I_{max1} == 0 : nomax1 = 0$ else $nomax1 = 1$. This condition is necessary for textures with only 2 non-zero intensity magnitudes.
- Repeat these steps for other texture classes by studying the intensities and their locations in the histograms and setting the parameters above accordingly.

The texture based feature learning approach outlined above is summerised in the flow diagram shown in figure 5.4.

5.3 Classification Algorithm

The input of the classification is a multi-object scenario that has not been encountered before. The entire image is passed into each class template for processing. The classification only require a constrained anisotropic diffusion filtering stage for noise removal and enhancement of the image. An object belonging to Class A, for example, is only visible if the template representing Class A features is applied, and so is for the rest of the classes. Any object in the multiple object scene belonging to a class other than that of the applied template is suppressed into a black background. The objects appear as a set of white pixels distributed in the multiple object image. Colour coding can also be

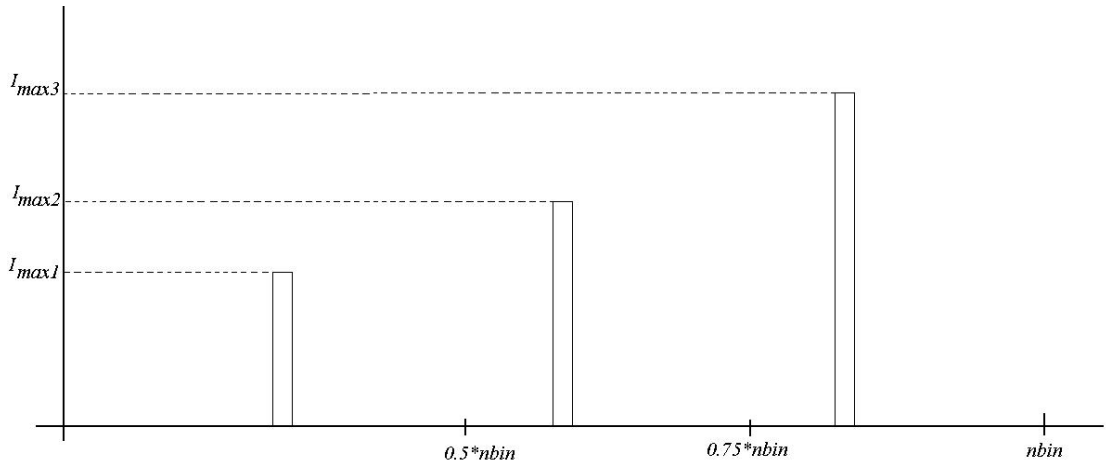

Figure 5.3: A Typical diffusion filtered histogram

used to mark objects belonging to one class.

As in the training algorithm for the first method proposed, the classification algorithm uses the associative CNN. The input image is applied to the network as a state image. In summary, the classification algorithm applies an input multiple object image into:

$$\dot{X} = -X + \sum T_A * Y + I_A \tag{5.1}$$

where X is the state image set to the input image ($X = U$), T_A and I_A are template parameters representing Class A and Y is a binary image representing the location of objects belonging to Class A as white pixels in a black background.

In the second method, the classification applies a histogram generator to get DF and MD histograms, and then uses the stored decision boundaries to classify the object. Thus, for a three class problem the classification algorithm generates three images from the multiple object input image, with each image showing a display of objects belonging to that class as a set of white pixels. The diagram in figure 5.5 represents the algorithmic and optical flows of this classification algorithm.

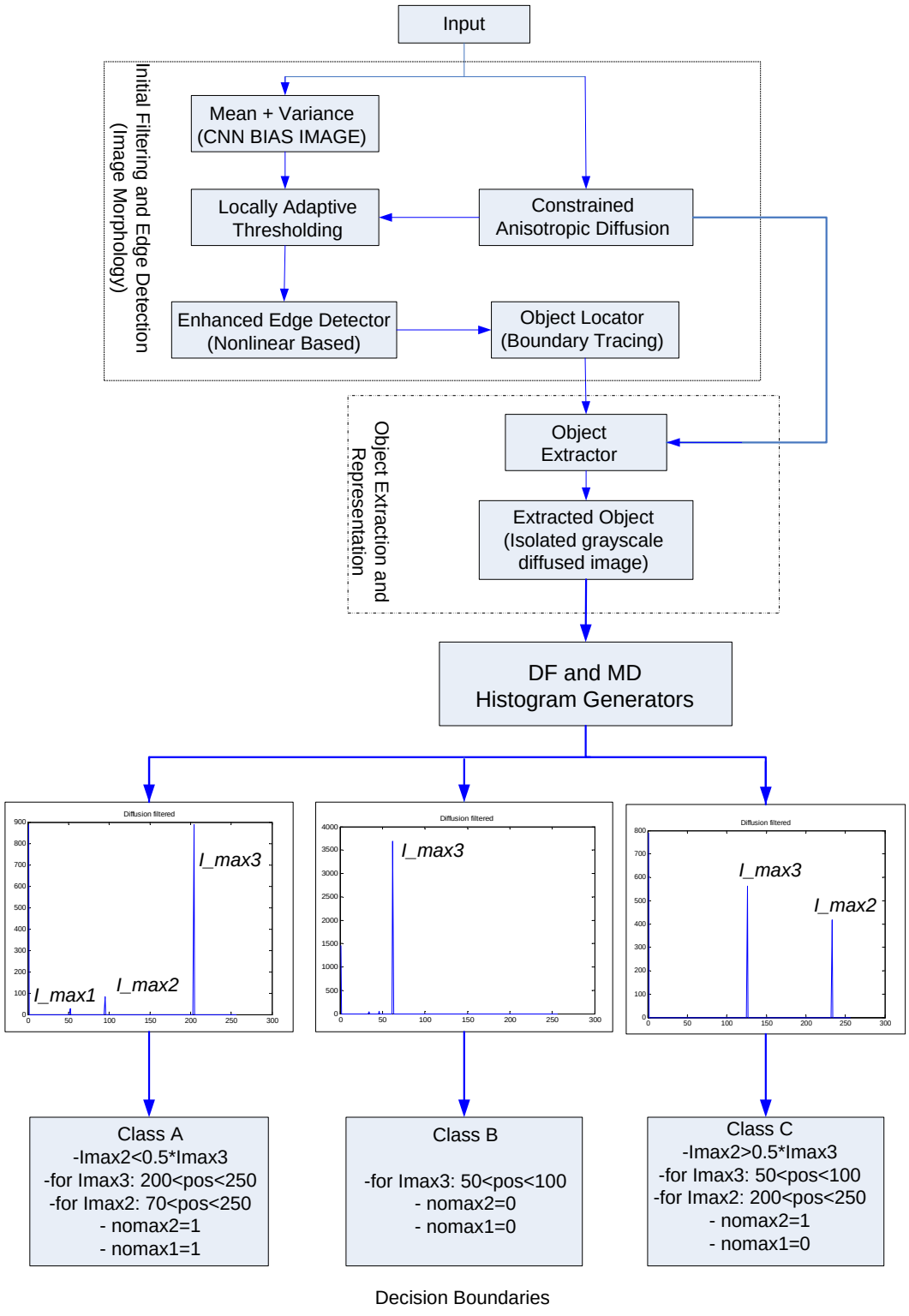

Figure 5.4: Flow diagram showing feature extraction and learning using diffusion filtered histograms

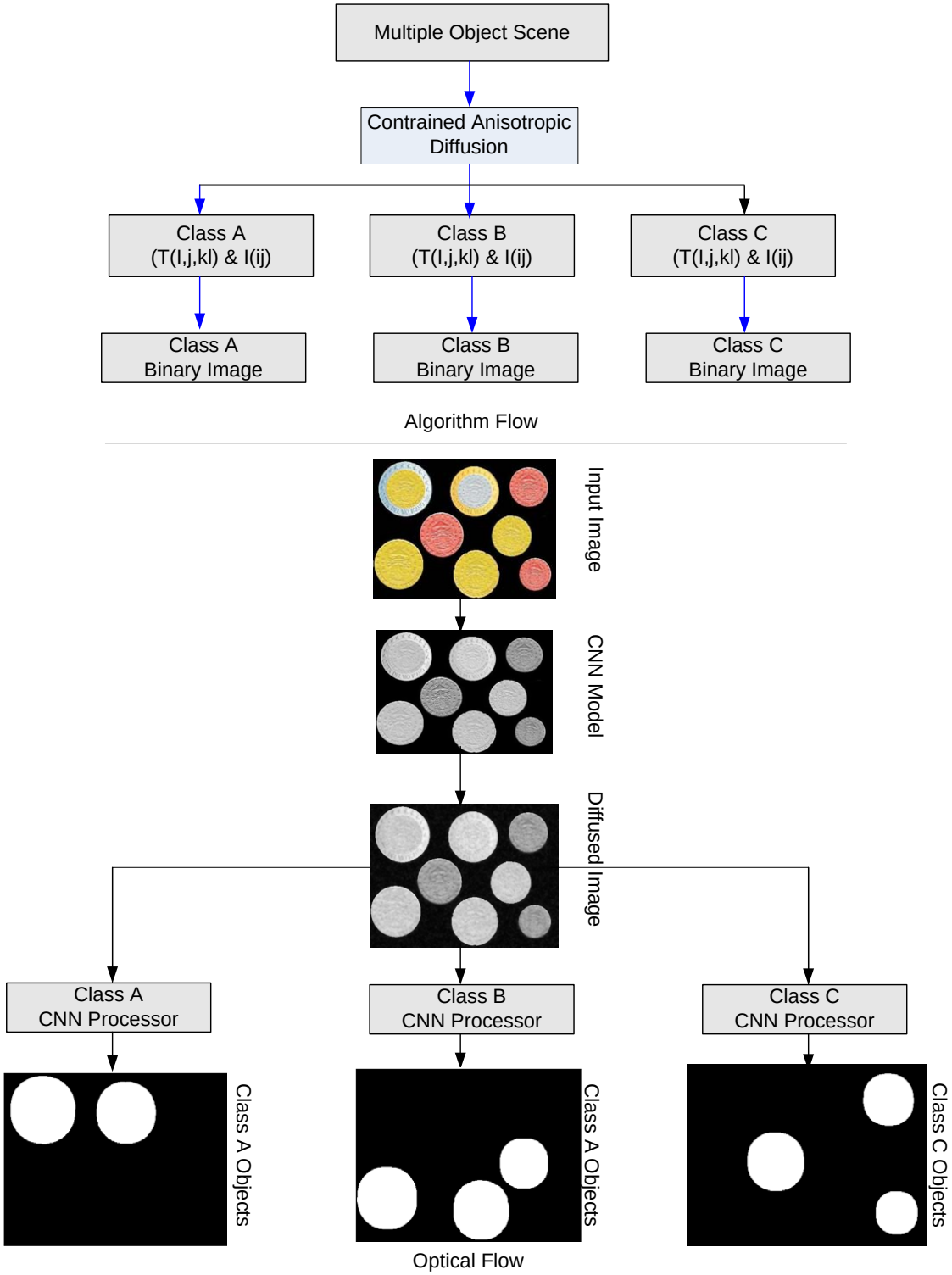

Figure 5.5: A proposed classification method using associative CNN

Chapter 6

Application Examples and Analysis

In this chapter, application examples using the proposed algorithms are presented. The first algorithm is applied to the field of satellite data modeling for landuse/cover classification purposes. In the resent past, there has been an increase in research for satellite data interpretation. This is due to the increasing need to study the global phenomena such as global warming, urbanization, climatic changes and land cover and land use pattern changes. This is also yielded by the cheap availability of satellite data for public use. Satellite sensing technologies have also improved significantly in the past, now yielding satellite sensors with very high spatial, spectral and temporal resolutions. Landsat have launched landsat 7 satellite that provides geographical data for the United States Geographical Survey (USGS). The second algorithm is applied to a scene with 4-class texture objects. The Histogram modification is done and the decision boundaries for each class are established. The objects are then classified using the boundaries formulated.

6.1 Application Example 1: Satellite Data Classification using Genetically Optimized CNNs

In this example the proposed method is applied to a landsat 7 scene in order to characterize and classify the land cover features of a scene located in the source of the Nile river, Jinja, Uganda. The purpose is to classify the scene features into built-up, vegetation and water areas. This example appears in [62] that was published during this research. The input image to the algorithm presented in figure 5.1 in the previous chapter is as shown in figure 6.1.

Figure 6.1: The source of the river nile, Jinja: 2001 Landsat 7 scene (row 171 and row 60) with built-up, vegetation and water areas [28]

The resulting cloning templates for each class as found from the algorithm are shown in equations 6.1 to 6.3. In the equations, T_B, T_V and T_W are the space invariant cloning templates generated by the GA algorithm for the built-up, vegetation and water areas respectively.

$$T_B(ij,kl) = \begin{pmatrix} -0.952 & -2.985 & 3.083 \\ 4.500 & 3.997 & 3.906 \\ -4.019 & 0.367 & 0.367 \end{pmatrix},\ I_B = \begin{pmatrix} -4.0305 \end{pmatrix} \tag{6.1}$$

$$T_V(ij,kl) = \begin{pmatrix} -1.198 & -5.587 & -5.035 \\ -1.430 & -3.997 & -0.063 \\ -3.024 & -5.556 & -6.003 \end{pmatrix},\ I_V = \begin{pmatrix} -5.654 \end{pmatrix} \tag{6.2}$$

$$T_W(ij,kl) = \begin{pmatrix} -3.520 & 3.111 & 3.282 \\ 1.543 & 2.835 & 2.352 \\ 1.690 & 1.540 & -0.845 \end{pmatrix},\ I_W = \begin{pmatrix} -7.9453 \end{pmatrix} \tag{6.3}$$

When these templates are applied to the input image in figure 6.1, the classification images shown in 6.2, 6.3 and 6.4 are found.

Figure 6.2: Extracted built-up areas using the proposed GA optimized associative CNNs

A possible application for this is in the field of environmental studies, wherein the relationships between different land cover features can be compared through images. Example of these relationships are depicted by images 6.5, 6.6 and 6.7 that can be used

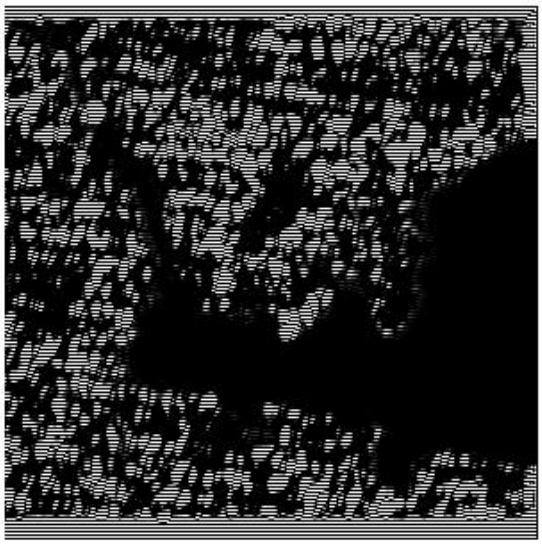

Figure 6.3: Extracted vegetation areas using the proposed GA optimized associative CNNs

Figure 6.4: Extracted water areas using the proposed GA optimized associative CNNs

to study the relationships built-up vs vegetation, vegetation vs water, and Build-up vs water respectively. These studies have yielding results in formulating regulatory laws for governing and monitoring the environment.

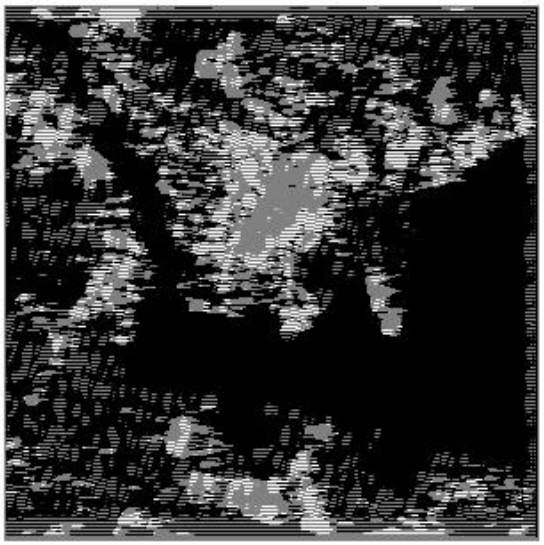

Figure 6.5: Built-up areas versus Vegetation areas

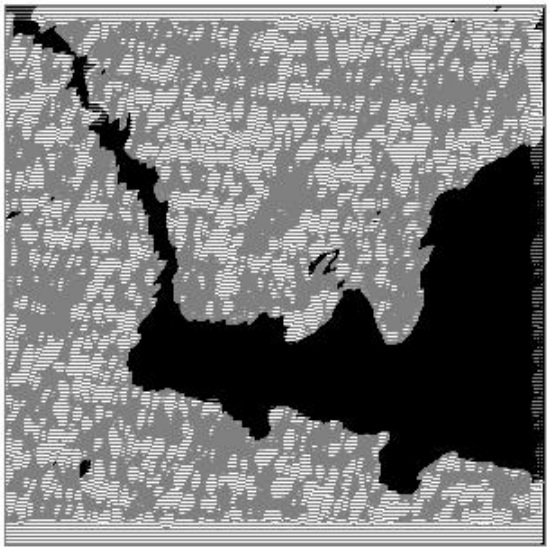

Figure 6.6: Vegetation areas versus Water areas

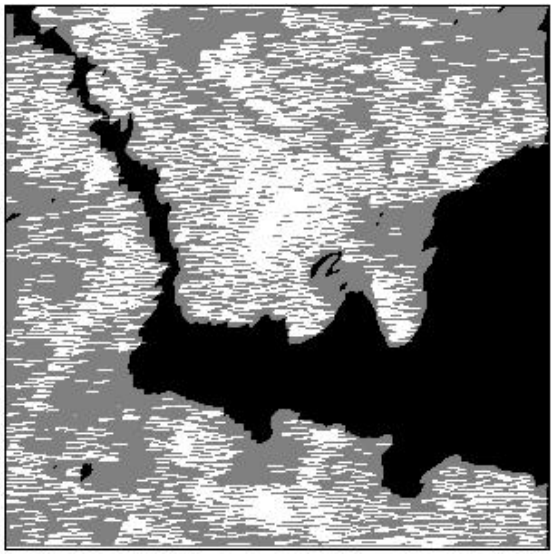

Figure 6.7: Built-up areas versus Water areas

6.2 Application Example 2: Texture Classification using DF and MD Histograms

Consider an image shown in figure 6.8. There are four texture classes in the image as shown by the arrows. The histograms representing each texture class are shown in figures 6.9, 6.10, 6.11 and 6.12.

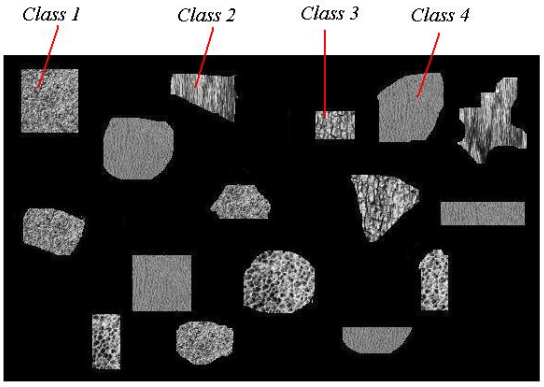

Figure 6.8: 4-Class Texture objects scene

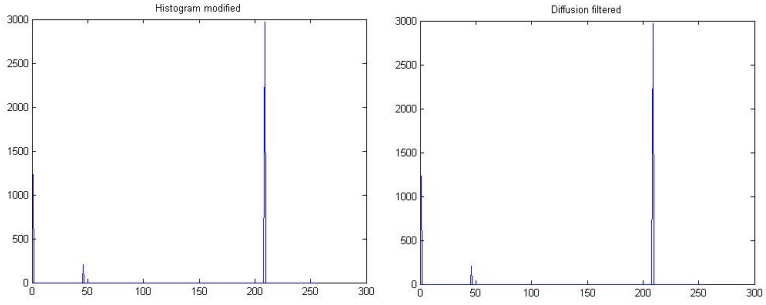

Figure 6.9: Class 1 MD and DF histograms

The classification images for each class are shown in figure 6.13. The objects that are circled in the images are those incorrectly classified.

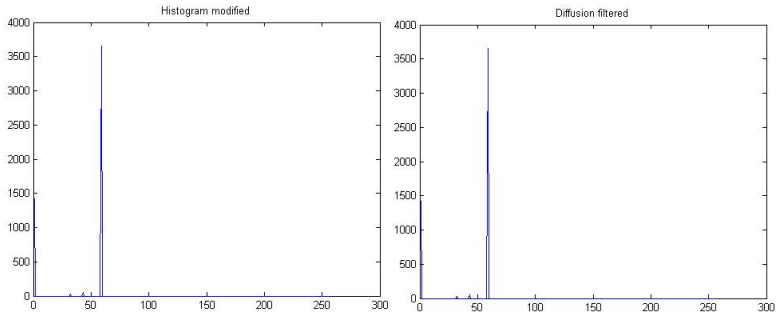

Figure 6.10: Class 2 MD and DF histograms

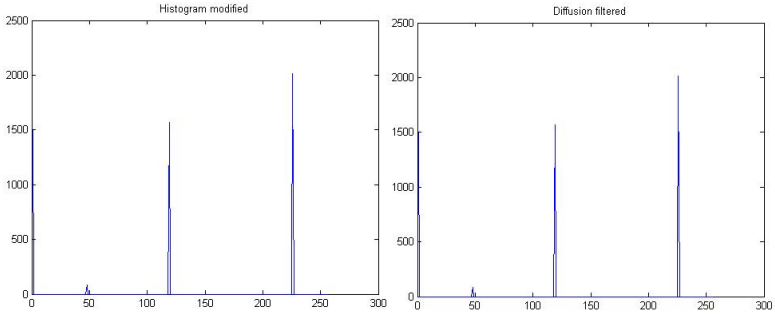

Figure 6.11: Class 3 MD and DF histograms

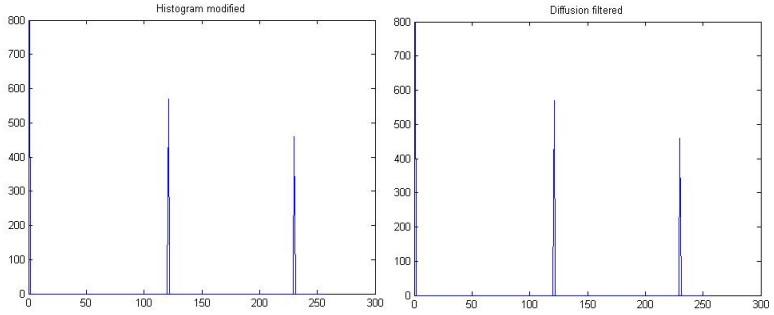

Figure 6.12: Class 4 MD and DF histograms

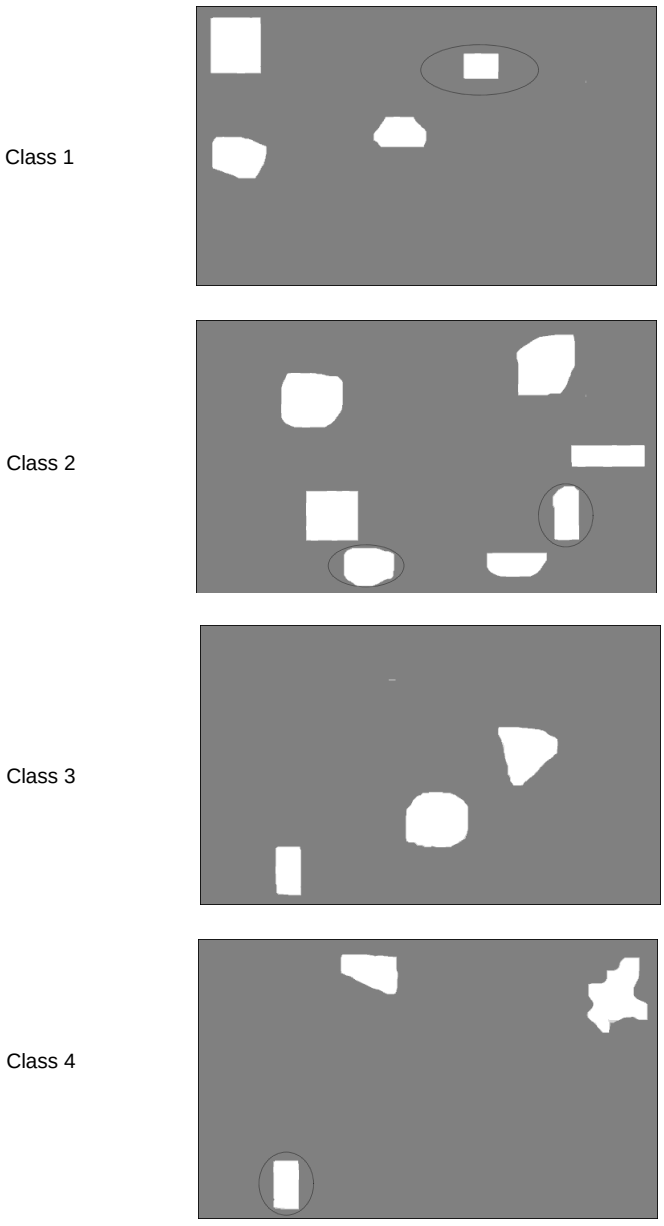

Figure 6.13: Classification images generated by decision boundaries based on DF and MD histograms

6.3 Analysis

Cellular Neural networks were introduced in Chapters 1 and 2 as a paradigm for complexity. In this dissertation, a method of computing and understanding the spatio-temporal properties of multiple object scenes was proposed, making use of CNNs as a platform for computing. This chapter attempts to justify the suitability of CNNs for spatio-temporal processing tasks through the analysis of the results from application examples presented in sections 6.1 and 6.2. First the analysis procedure to be used is presented, followed by the analysis of results from each example. The last section draws the differences between CNN architectures and a well-known Hopfield network as a way of demonstrating a number of advantages inherent in the use of the CNN the model in spatio-temporal processing.

6.3.1 Analysis Procedure

In this section, the procedure to evaluate the performance of the solution proposed for multiple object scenario is developed. The following aspects will be considered to develop an analysis procedure:

- **Architectural Efficiency** - This test will measure the efficiency of the architecture used in modeling the problem that this research has embarked to solve. The aspects of architecture that are of concern are the simplicity of the model, integration suitability for on-chip spatio-temporal solutions, scalability and synchronous processing.

- **Memory efficiency and learning ability** - This procedure will evaluate the computational speed for both learning and classification algorithms.

- **Processing Accuracy and Efficiency** - Here the error rate of the proposed solution is measured and the efficiency of the algorithm calculated based on the application example presented in Chapter 6.

- **Comparison with other network architectures** - In this procedure the CNN is compared with its counterparts based on established theories and limitations

6.3.2 Analysis of the Results

(a). The Architectural Efficiency of the CNN Model

CNNs are analog processors. In comparison with their digital counterparts, analog processors have been found to be very fast computers. The challenge in analog processing is to establish decision rules based on signal levels. CNNs achieve this by using logic rules that are common to digital processing. Thus, CNNs provide the best of both worlds, i.e the fast processing speed of the analog world, and the accurate decision rules of the digital world. Each single cell of the CNN is a processing unit, which means that more data can be processed faster all at once. This puts CNNs in a good position in the race to parallel processing. CNNs are based on local processing, requiring only few data to be stored to achieve the model. The local processing nature puts cellular neural networks as ideal candidates for on-chip Very Large Scale Integration (VLSI).

(b). Memory Usage and Learning Ability

Assuming a common AB-type network based on a 3 x 3 template, there are only 19 elements that require permanent storage in the CNN representation. These are the A, B, and I kernel matrices that defines the behaviour of the network. However, a network adopted for processing multiple object scenarios in this research is an associative network which only requires 10 elements of the kernel matrix for representation. This further reduces the memory usage, making the CNN the most ideal candidate for on-chip integration. Also, the processing power of this network is two-fold. On one hand there is its analogic nature, and on the other there is the parallelism. The combination of these makes the CNN model have the computing power of a supercomputer.

With little memory required for CNN model representation, the CNN still possess a high learning ability. This is achieved by developing only local interactions that best represent the overall behavior of the network. The a 3x3 CNN is normally enough to capture the most distinguishing features of the object. The graph in figure 6.14 shows the learning curves for the GA-based learning algorithm in the application example presented in chapter 6.

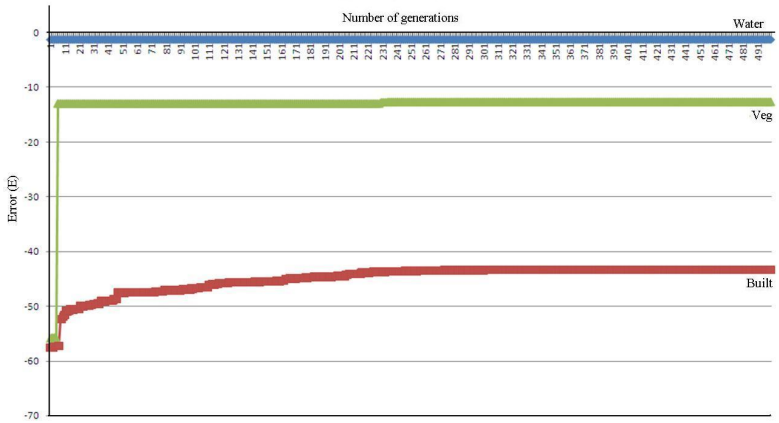

Figure 6.14: Learning curves of the GA-based algorithm

(c). Processing Accuracy and Efficiency of the Model

Using the results from the application example in sections 6.1 and 6.2, the classification error can be calculated. By mapping the classification images generated by the algorithm proposed the number of pixels incorrectly classified can be obtained. The mappings are done by computing images that represent the relationships "builtup vs vegetation", "vegetation vs water" and "builtup vs water images". From these relationships, an image that represent clashing pixels is generated. Pixel clashes in the relationship images represent a classification error from either one of the classifier templates belonging to the classes being compared. The images in figures 6.15, 6.16 and 6.17 show the error pixels in black and their exact locations in the input study image.

The number of error pixels per each comparison of the classification images is as follows:

-Builtup Area VS Vegetation Area = 2189 error pixels
-Vegetation Area VS Water Area = 1734 error pixels
-Builtup Area VS Water = 48 error pixels

From the error pixels, the classification error of the algorithm can be calculated. By

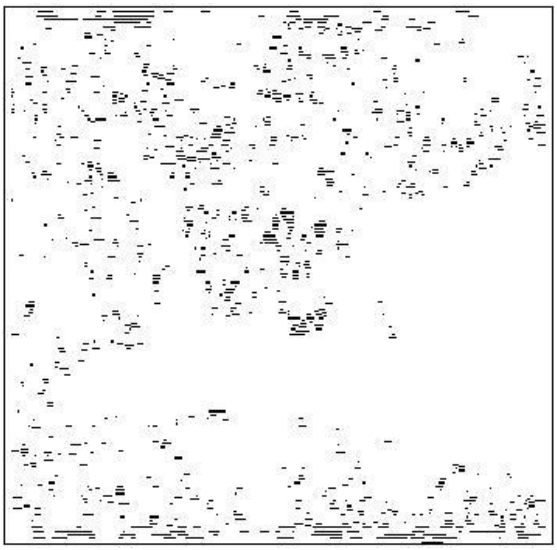

Figure 6.15: Error pixels in the classification of Built Area vs Vegetation Area

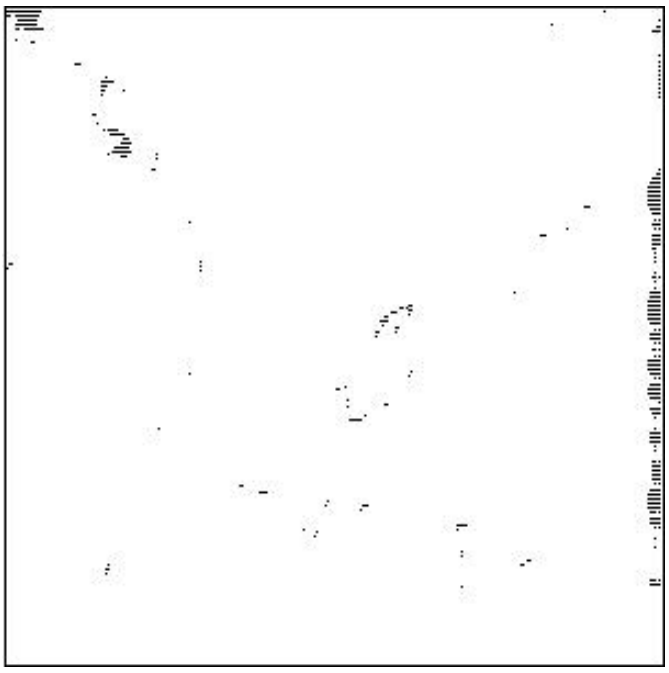

Figure 6.16: Error pixels in the classification of Vegetation Area vs Water Area

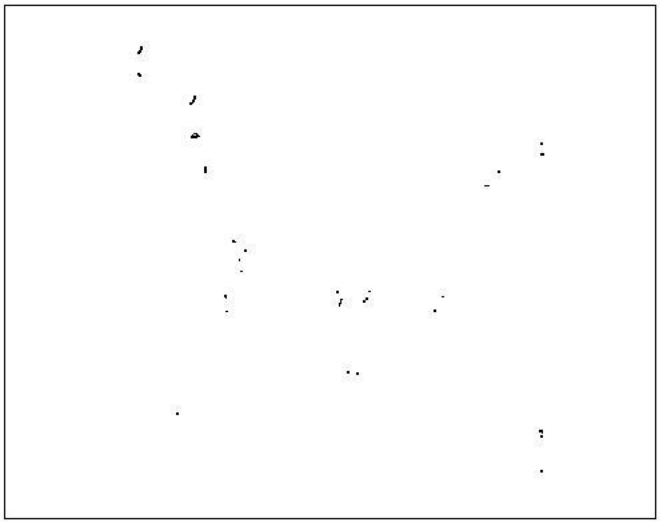

Figure 6.17: Error pixels in the classification of Built Area vs Water Area

labeling these pixels as error pixels in the image, it is automatically implied that all the other pixels in the image are correctly classified, so the classification error is then calculated as the percentage of the error pixels in the total image as follows:

1. Built vs Vegetation

$$\%\ error = (\frac{no.\ of\ error\ pixels}{Total\ image\ pixels}) * 100 = \frac{2189}{90601} * 100 = 2.4\%$$

2. Vegetation vs Water

$$\%\ error = (\frac{no.\ of\ error\ pixels}{Total\ image\ pixels}) * 100 = \frac{1734}{90601} * 100 = 1.91\%$$

3. Builtup vs Water

$$\%\ error = (\frac{no.\ of\ error\ pixels}{Total\ image\ pixels}) * 100 = \frac{28}{90601} * 100 = 0.03\%$$

4. Thus, from the error estimations in points 1, 2 and 3 the overall efficiency is calculated as

$$\%\ efficiency = 100 - \frac{2.4 + 1.91 + 0.03}{3} = 98.6\%$$

In view of the results shown by error and efficiency calculations, it can be concluded that CNNs optimized with GAs are well suited to the spatio-temporal classification problems. It is also important that this accuracy is achieved with reduced architectural complexity, increased computational speed, one-to-one mapping between pixels and neurons and a cheap analog circuit ready for on-chip integration.

6.3.3 Efficiency of the texture-based approach

The efficiency of classification of textures based on histograms is hindered by the lack of a more precise method of comparing histograms. The task of designing boundary conditions for each class is done as a manual process. This may not be accurate as the performance is highly dependent on the ability of the designer to capture global relationships between objects of same textures. There is a need to design an AI based tool for capturing the histogram relationships that govern a class of objects with a certain texture. This method will eliminate locally optimal designs and the errors introduced by the use of common heuristics in the class designs. However, classification of object based on textures remain a very effective tool provided that accurate boundary conditions are captured from the histograms.
From the results provided in section 6.2, it is has been shown that the method is effective as 4 out of 15 objects were correctly classified. By redesigning the bounds to represent the global behaviour of texel intensities per area, all objects can be correctly classified.

6.4 Comparison with other Network Models

We now compare the CNN model that was studied and applied in this dissertation with the well known Hopfield model. This is done in the spirit of demonstrating some advantages of the CNN model over the hopfield architecture in spatio-temporal processing. Below are some few comparisons that can be drawn between the CNN and the Hopfield model.

Table 6.1: Comparison of the CNN and the Hopfield Models.

Area	**CNN**	**Hopfield**
Network Connectivity	Local	Global
Operating mode	Synchronous mode	Asynchronous
Associative Memories	Coupling rules set by template synthesis procedures or Optimization	Weights are computed by the Hebb rule
Processing Circuitry	Analog circuit	Digital Circuit
Processing Elements	Cells	Nodes
Spatio-temporal Mapping	One-to-one with image pixels	Depends on representation
Number of Inputs vs Network Nodes	A CNN of $n = NXM = 9\ for\ M = N = 3,\ r = 3$ has a total of 289 interconnections	A Hopfield Network of $n = 9$ has a total of 729 interconnections
Template symmetry	No assumption about template symmetry	Template is required to be symmetric

Chapter 7

Conclusion, Discussions and Recommendations

7.1 On Suitability of the CNN to Spatio-temporal Processing

Using the CNN model, it has been illustrated in this dissertation that a complex system can be modeled using an associative network. The model only requires few elements and is mathematically easy. Through achieving the model of a cell that best represent the data structure and its patterns in the network, a complex environment is reduced into a model easy to understand and compute. In this dissertation, we chose autonomous CNNs as the platform for modeling the spatio-temporal properties of objects. The model has led to a proper extraction of the objects and the ease of formulation for learning methods. An accuracy of 98% in the classification problem outlined in section 6 indicates that these networks have high performance in spatio-temporal environments. There is also a notable difference in structural constituents between the CNNs and the Hopfield as tabulated in Table 6.1 of section 6. This has yielding factors in terms of computational speed, memory usage and implementation difficulties. These further motivates the adoption of CNNs by many researchers as an image processing platform. Through this research, the powerful processing nature of the CNN has been demonstrated.

7.2 On Feature Learning and Classification

Like any other network, the CNN performance in classification also require further optimization to terminate at a global solution for each class of objects. This document has proposed the use of Genetic Algorithms to optimize autoassociative CNNs to perform learning of spatio-temporal features. It is important to note that most of the feature learning algorithms known in research are instructed by a user program to capture certain specific features (measured through mathematical computations) of the object. The proposed algorithm using GAs in this research does not make this assumption. It however allows the learning algorithm to extract any feature(s) from the object that best distinguish it from the rest. This presents an advantage in cases where there may not be a better mathematical model for extracting features. We single out one statistical feature extractor that is worth noting, this is the texture histograms. Though this method requires a lot of manual computations in forming decision boundaries for object classes, it remains effective. With accurate class design all the objects in a multiple object scene can be correctly classified.

The efficiency of the CNN network also lies in the ability to implement analogic algorithms. This means that certain templates required in more than one processing stages can be reused whenever the need arise. These analogic algorithms take place at pixel level and hence are applied in accordance with the required or existing coupling rules on the network. This very nature of CNNs makes them more easier to design and scale according to the application requirements.

7.3 Research Contribution

This section serves as a reaffirmation of the contributions stated in section 1.4. The algorithms developed on chapters 4 and 5 yield a solution which reduces model complexity, increases the computational speed as well as the easy-to-implement training algorithm for samples to be detected. This document has outlined various advantages of CNNs over classic image processing methods. Also, this research work has also addressed a solution of modeling with multiple image scenes. By learning each object from its surrounding environment (i.e. in a multiple image scene of its existence), the object appearing in a multiple image scene can be easily detected and classified. The solutions

proposed in this research are applicable to industrial processing tasks such as visual quality inspection, surveillance and monitoring as well as geographical data analysis. This research proposes an efficient way of handling scenes with more than one object belonging to different classes.

7.4 Future Work and Recommendations

Though the algorithm proposed in this dissertation was reported to be efficient, there are areas of concern that require further research. The accuracy of Genetic Algorithms has shown a decrease when the need to use templates with neighbourhoods greater than 2 arise. While templates with more parameters may capture more data on the input, they cannot be optimized using GAs unless the parameters are reduced by setting some to constant values. Setting some parameters to constant values may sacrifice the template's feature capturing abilities, while leaving them as variables for GA optimization may result in a large GA solution space that may not terminate at optimal templates. Arriving at a trade-off between these two is a matter of further research.

There is also the need to devise a standardized method for histogram comparisons in texture-based feature extractions. Histograms provide more important aspects about textures on the image, thus a better way of establishing texture classes will be in support of the strength of histograms in this field.

References

[1] L. Fortuna, P. Arena, D. Balya and A. Zarandy, "Cellular Neural Networks: A Paradigm for Nonlinear Spatio-temporal Processing", *Circuits and Systems Magazine, IEEE*, Vol. 1, Issue: 4, 2001, pp. 6-21.

[2] O. V. de Paul, "Remote Sensing: New Applications for Urban Areas", *Proceedings of the IEEE*, Dec. 2007, Volume 95, Issue 12, pp. 2267 - 2268.

[3] M. H. ter Brugge, R. J. Krol, J. A. G. Nijhuis, L. Spaanenburg, "Design of Discrete-Time Cellular Neural Networks Based on Mathematical Morphology", *Proceedings of the fourth IEEE International Workshop on Cellular Neural Networks (CNNA-96), Seville (Spain)*, June 1996, pp. 1-5.

[4] L. Spaanenburg *et al*, "Natural learning of neural networks by reconfiguration", *Proc. SPIE, Bioengineered and Bioinspired Systems*, Vol. 5119, April 2004, pp. 273-284

[5] L. O. Chua and L. Yang, "Cellular Neural Networks: Theory", *IEEE Trans. On Circuits and Systems*, Vol. 35, No. 10, October 1988, pp. 1257-1272.

[6] L. O. Chua. "CNN: A Paradigm for Complexity", *World Scientific Series on Nonlinear Science*,Vol 1, Series A, June 1998.

[7] L. M. Lederman and D. N. Schramm, "From Quarks to the Cosmos: Tools of Discovery", volume 28 of Scientific American Library Series. W.H. Freeman and Company, 1995. [8] L.O. Chua and T. Roska, Cellular Neural Networks Paradigm, *IEEE Trans. on Circuits and Systems I: Fundamental Theory and Applications*, Vol. 40, No. 3, Mar 1993, pp. 147-156.

[9] S. Xavier-de-Souza, J. A. K. Suykens, and J. Vandewalle. "Learning of Spatiotemporal Behavior in Cellular Neural Networks". *International Journal of Circuit Theory and Applications - Special Issue on CNN Technology (Part 1)*, 34:127140, Jan 2006.

[10] L.O. Chua and T. Roska, Cellular neural networks and visual computing, Foundations and applications (Cambridge UK: Cambridge University Press, 2002) 205-231.

[11] M. G. Milanova, A. Elmaghraby, S. Rubin, "Cellular Neural Networks for Segmentation of Image Sequence", *Journal on Neurocomputing*, Vol. 31(1-4), 2000, pp. 125-141.

[12] W. Aziz and T. Lala, "Controllability, Applications, and Numerical Simulations of Cellular Neural Networks", *2003 Colloquium on Differential Equations and Applications*, Maracaibo, Venezuela. Electronic Journal of Differential Equations, Conference 13, 2005, pp. 111.

[13] J. Austin, "The cellular neural network associative processor, C-NNAP", *Fifth International Conference on Image Processing and its Applications*, 1995, pp. 622-626.

[14] P. Szolgay, I. Szatmari, and K. Laszlo, "A Fast Fixed Point Learning Method to Implement Associative Memory on CNNs", *Circuits and Systems I: Fundamental Theory and Applications, IEEE Transactions on Circuits and Systems I*, Vol. 44, Issue 4, Apr 1997, pp. 362-366.

[15] Z. Lu and D. Liu, A New Synthesis Procedure for a Class of Cellular Neural Networks with Space-Invariant Cloning Template, *IEEE Trans. on Circuits and Systems IIAnalog and Digital Signal Processing*, Vol. 45, No. 12, December 1998.

[16] T. Roska, K. Lotz, J. Hamori, E. Labos, and J. Takacs, "The CNN model in the visual system", Part 1: The CNN-retina and some direction and length-selective mechanisms, Research Report of the Analogic (Dual) and Neural Computing Systems Laboratory (DNS-8-1991), Budapest, MTA SZTAKI.

[17] J.L. Teeters F.S. Weblin, "Real-time simulation of retina allowing visualization of each processing stage",*SPIE*, 1472. [18] T. Roska, "Cellular Wave Computers for Brain-like Spatial-temporal Sensory Computing", *IEEE ISCAS 2004 Plenary Lecture*, Vancouver, May, 2004.

[19] Y. Wang, W. Zhou and X. Wang, "Cellular Neural Networks for Object Segmentation of Image Sequence", *Asian Journal of Information Technology* , Vol. 4(11), 2005, pp. 1098-1101.

[20] T. Szabo and P. Szolgay, "Analogic Diffusion-Based Algorithm for the segmentation of CT/MRI Images",*Circuit Theory and Design. Proceedings of the 16th European Conference ECCTD'03*, Vol. 1, 2003, pp. 237-239.

[21] C. Rekeczky, "Adaptive Multi-rate, Multi-grid and Multi-scale Algorithms Running on Analogic Architecture",*Circuit Theory and Design. Proceedings of the 16th European Conference ECCTD'03.* Vol. 1, 2003, pp. 404-404.

[22] D. Balya, T. Gergely, I. Szatmari, and C. Rekeczky, "Classification of Spatio-Temporal Features: The Nearest Neighbor Family", *The 16th European Conference on Circuits Theory and Design, ECCTD'03*, Vol. 3, 2003, pp. 129-132.

[23] D. Balya, G. Timar, I. Szatmari, and Cs. Rekeczky, "Efficient Off-line Feature

Selection Strategies for On-line Classifier Systems", *in Proc. of the IEEE Int. Joint Conference IJCNN'04*, Vol. 1, 2004, pp. 171-176.

[24] F. Dellaert and J. Vandewalle, "Automatic Design of Cellular Neural Networks by means of Genetic Algorithms: Finding a Feature Detector", *in Proc. IEEE Int. Workshop on Cellular Neural Networks and Their Applications*, 1994, pp. 189-194.

[25] O. Dekhtyarenko, A. Reznik and A. Sitchov, "Associative Cellular Neural Networks with Adaptive Architecture", *In proc. of The 8th IEEE International Biannual Workshop on Cellular Neural Networks and their Application (CNNA'04), Budapest, Hungary*, July 2004, pp. 219-224.

[26] C. K. I. Williams and M. K. Titsias. "Learning about multiple objects in images: Factorial learning without factorial search". *Advances in Neural Information Processing Systems*,2003, pp. 1415-1422.

[27] Williams, C. K. I. and Titsias, M. T. (2003). Learning about multiple objects in images:Factorial learning without factorial search. In Becker, S., Thrun, S., and Obermayer, K., editors, Advances in Neural Information Processing Systems. MIT Press.

[28] R. Simmon, "NASA image based on Landsat-7 data provided by the UMD Global Land Cover Facility". U.S Geological Survey, Internet Listing, Last accessed: 17 December 2008, Last updated: 22 Sep 2008,
http://earthobservatory.nasa.gov/IOTD/

[29] A. Schultz, C. Rekeczky, I. Szatmri, T. Roska, and L.O. Chua, "Spatio-temporal CNN Algorithm for Object Segmentation and Object Recognition", *5th IEEE Int. Workshop on Cellular Neural Networks and their Applications (CNNA-98)*, pp. 347-352, London, April 14-19, 1998.

[30] C. Rekeczky, "Analogic CNN Simulation Toolbox for MATLAB", *Analogical and Neural Computing Laboratory,Computer and Automation Institute, Hungarian Academy of Sciences*,H-1111 Budapest, Kende u. 13-17.

[31] T. Boros, K. Lotz, A. Radvnyi, and T. Roska, Some Useful New Nonlinear and Delay-type Templates, *Research report of the Analogical and Neural Computing Laboratory, Computer and Automation Research Institute, Hungarian Academy of Sciences (MTA SzTAKI)*, DNS-1-1991, Budapest, 1991.

[32] H. Harrer, P. L. Venetianer, J. A. Nossek, T. Roska, and L. O. Chua, "Some Examples of Preprocessing Analog Images with Discrete-Time Cellular Neural Networks", *Proceedings of the International Workshop on Cellular Neural Networks and their Applications (CNNA-94)*, pp. 201-206, Rome, 1994.

[33] J. Weickert,"Anisotropic diffusion in image processing", *ECMI Series*, Teubner, Stuttgart, 1998. ISBN 3-519-02606-6.

[34] P. Perona and J.Malik, "Scale-Space and Edge Detection Using Anisotropic Diffusion", *IEEE Trans.on PAMI*, Vol. 12, July 1990, pp. 629-639.

[35] D. Keysers and C. H. Lampert and T. M. Breuel, "Color image dequantization by Constrained Diffusion",*SPIE Electronic Imaging*, 2006.

[36] J. Weickert, Applications of Nonlinear Diffusion In Image Processing and Computer Vision, *Proceedings of Algoritmy 2000. Acta Math.*, Univ. Comenianae Vol. LXX, 1(2001), pp. 3350.

[37] M. J. Black, G. Sapiro, D. H. Marimont,and D. Heeger, "Robust Anisotropic Diffusion", *IEEE Trans on Image Processing*, VOL. 7, NO. 3, MARCH 1998.

[38] T. Sziranyi and M. Csapodi, Texture Classification and Segmentation by Cellular

Neural Networks Using Genetic Learning, *Computer Vision and Image Understanding*, Vol. 71, No. 3, September 1998, pp. 255-270.

[39] Cs. Rekeczky, T. Roska, and A. Ushida, "CNN-based Difference-Controlled Adaptive Nonlinear Image Filters", *International Journal of Circuit Theory ans Applications*, Vol 26,1998, pp 375-423.

[40] L. Nemes, L. O. Chua, and T. Roska, "Implementation of Arbitrary Boolean Functions on the CNN Universal Machine", *International Journal of Circuit Theory ans Applications*, Vol 26 (6), 1998,pp 593-610.

[41] T. Roska, L. Kk, L. Nemes, and . Zarndy (ed),"CNN Software Library (Templates and Algorithms) Version 7.0", Research report of the Analogic (Dual) and Neural Computing Systems Laboratory, (DNS-1-1997), Budapest MTA SZTAKI, 1997.

[42] M. Gilli, "Template Design Methodologies and Tools", *European Conference on Circuit Theory and Design - ECCTD'99, Design Automation Day proceedings, (ECCTD'99-DAD)*, pp. 113-126, Stresa, Italy, 1999.

[43] . Zarndy, "The Art of CNN Template Design", *Int. J. Circuit Theory and Applications - Special Issue: Theory, Design and Applications of Cellular Neural Networks: Part II: Deign and Applications*, (CTA Special Issue - II), Vol.17, No.1, pp.5-24, guest ed: T. Roska, A. Rodriguez-Vazquez and J. Vandewalle, 1999,

[44] B. Mirzai, D. Lim, G.S. Moschytz, "Robust CNN Templates: Theory and Simulations", *Proceedings of IEEE Int. Workshop on Cellular Neural Networks and Their Applications, (CNNA'96)*, pp.393-398, Sevilla, 1996,

[45] K. R. Crounse and L. O. Chua, "Methods for image processing and pattern formation in cnn:A tutorial." 42, no. 10, (1995),pp 583601.

[46] Leon O. Chua and L. Yang, "Cellular neural networks: Applications", *IEEE. Transc. Circuits Syst. 35 (1988)*,pp 12731290.

[47] P. Liu, N. Wu, J. Zhu, J. Yin, and W. Zhang, "A Unified Strategy of Feature Selection",*Lecture Notes in Computer Science, Advanced Data Mining and Applications*, Vol 4093, July 2006, pp. 457-464.

[48] M. Tuceryan and A. K. Jain, "Texture Analysis",*The Handbook of Pattern Recognition and Computer Vision (2nd Edition)*, Chapter 2.1, pp. 207-248, World Scientific Publishing Co., 1998.

[49] B. E. Shi and K. Boahen, "Competitively Coupled Orientation Selective Cellular Neural Networks", *IEEE Trans. On Circuits and SystemsI: Fundamenta Theory and Applications*, VOL. 49, NO. 3, MARCH 2002.

[50] D. Liu and A. N. Michel, "Dynamical Systems with Saturation Nonlinearities: Analysis and Design", *New York: Springer-Verlag*, 1994.

[51] D. Liu and A. N. Michel, "Sparsely interconnected neural networks for associative memories with applications to cellular neural networks", *IEEE Trans. Circuits Syst. II*, vol. 41, pp. 295309, Apr. 1994

[52] D. Liu and A. N. Michel, "Robustness analysis and design of a class of neural networks with sparse interconnecting structure", *Neurocomputing*, vol. 12, pp. 5976, June 1996.

[53] R. A. Hummel, "Histogram Modification Techniques", *Computer Graphics and Image Processing*, vol. 4, 1975, pp.209-224.

[54] K. J. Dana, B. Van Ginneken, S. K. Nayar, and J. J. Koenderink, "Reflectance and Texture of Real World Surfaces", *ACM Transactions on Graphics (TOG)*, Vol.18, No.1,

pp.1-34, Jan, 1999. Accessed via "The Columbia Image Database, CuRRET:Columbia-Utrecht Reflectance and Texture Database",
URL:http://www1.cs.columbia.edu/CAVE/exclude/curet/dataComp/, Last updated: 1999, Last Accessed: 17 December 2008.

[55] D.E. Goldberg, Genetic Algorithms in Search, Optimization, and Machine Learning, *Reading, Mass: Addison-Whesley*, 1989.

[56] Z. Michalewicz, Genetic Algorithms + Data Structures = Evolution Programs, *AI Series Springer Verlag*, New York, 1994.

[57] H. Bersini and B. Renders, "Hybridizing genetic algorithms with hill-climbing methods for global optimization - Two possible ways", *In 1994 IEEE International Symposium on Evolutionary Computation*, Orlando, Fl, 1994, pp. 312 -317.

[58] C. R. Houck, J. Joines, and M. Kay, "A genetic algorithm for function optimization: A Matlab implementation". *ACM Transactions on Mathmatical Software*, Submitted 1996.

[59] T. Kozek, T. Roska, and L. O. Chua, "Genetic algorithm for CNN template learning", Memorandum UCB/ERL, M92/82, Berkeley University of California at Berkeley, 1992,

[60] K. R. Crounse and L. O. Chua, "Methods for image processing and pattern formation in cnn: A tutorial. 42", no. 10, (1995), pp.583 - 601.

[61] M. Tanaka, K. R. Crounse and T. Roska, "Template Synthesis of Cellular Neural Networks for Information Coding and Decoding",*Proceedings of IEEE Int. Workshop on Cellular Neural Networks and Their Applications*, (CNNA'92),Munich, 1992, pp.29-35.

[62] T.C. Malumedzha and T. Marwala, "Classification of Satellite Sensed Data using Genetically Optimized Auto-associative Cellular Neural Networks",*From Proceeding (633) Intelligent Systems and Control - 2008*, November 2008, Orlando, USA, Accepted for publication.

[63] K. Mikolajczyk, "Multiple Object Class Detection with a Generative Model", *Proceedings of the 2006 IEEE Computer Society Conference on Computer Vision and Pattern Recognition - Volume 1*, IEEE Computer Society, 2006, pp. 26 - 36.